The completion of this thesis
was supported by the
Randy Seeling Award
given, in his memory, to another
outstanding graduate student
of the Geology Department,
University of Minnesota, Duluth.

HIGH GRADE METAMORPHISM AND PARTIAL MELTING IN THE BLUEGRASS CREEK SUITE, CENTRAL LARAMIE MOUNTAINS, WYOMING

A Thesis submitted to
the Faculty of the Graduate School of the
University of Minnesota

BY

MICHAEL JOSEPH SPICUZZA

In Partial Fulfillment
of the Requirements for the Degree of
Master of Science

March, 1990

ACKNOWLEDGEMENTS

I would like to acknowledge funding for this project received from the University of Minnesota-Duluth Geology Department and from the National Science foundation through a grant to Dr. James A. Grant (NSF #EAR 8409664). In addition, would like to thank Mr.and Mrs. Ken Seeling for supporting the geology department by setting up a fund to assist graduate students with the costs incurred during final preparation of the thesis. I respectfully acknowledge and thank the faculty and staff of the Department of Geology at the University of Minnesota-Duluth for making higher education academically rewarding in an amiable atmosphere.

I thank my committee members Dr. J.C. Nichol, Dr. J.C. Green, and Dr. J.A. Grant for their careful reviews and inciteful suggestions on the manuscript.

I thank Dr. James A. Grant for acting as my principle advisor, for suggesting this project and introducing me to the perplexing world of pelitic migmatites. His enthusiasm for migmatites was contagious, his incites most helpful, encouragement most needed, and friendship most appreciated.

I would like to recognize the members of the FLAC camp (Friends of the Laramie Anorthosite complex) including Dr. B.R. Frost, Dr. D.H. Lindsley, Ivan Carl Anderson, and the others who made the days in the booming metropolis of Laramie both educational and enjoyable. In addition I thank the land owners who allowed access to their property and to the owners of the Shamrock, who, in the land of air toast, supplied much needed supercooled fermented malt beverages to those desperate enough to be travelling state route 34 in Wyoming.

Dr. G.L. Snyder of the United States Geological Survey provided incite about and tours of the central Laramie mountains. In addition, this scotch drinking cribbage player is thanked for his unending hospitality and an unforgettable evening of trout fishing.

I would like to thank the undergraduate students in geology at the University of Minnesota-Duluth upon whom I was allowed to impose *my* interpretation of rocks. In addition, they taught me to enjoy broomball and the art of steelhead fishing.

I wish to thank the my fellow graduate students at UMD, through whom I learned much. In particular I thank W. James Dunlap for showing me the advantage of working late (ie. hitting last call), working hard (decent grades) and canoeing Quetico in early June (trophy bronzebacks).

I thank the faculty at Southern Methodist University for their patience in allowing me to continue my graduate education while working out the last few wrinkles in this thesis.

I thank Ms. Kathryn Arrington for her patience, her backrubs, her love and her ability to recognize "sentences" I have written which should (could?) never be read.

I wish to convey my gratitude to my parents, Frank and Nancy, who after years of hearing me grumble about school, watched quietly as I dove back in for more. Without their love and support, I do not believe I would have had enough confidence to undertake graduate school.

Finally, I wish to thank the Lord, for as I look back over this project I am amazed at all the wondrous places I have been and all the good friends I have made since entering graduate school. And to think, I could be fighting rush-hour traffic in Chicago 5 days a week, working in an office 50 weeks a year...

ABSTRACT

The Bluegrass Creek Suite (BCS) comprises Archean metasupracrustal rocks which suffered at least two periods of high grade metamorphism during the Precambrian. The first, a regional amphibolite grade metamorphism (6.0 kb, 660°C; Grant & Frost, 1986) at approximately 2.6 BY significantly dehydrated the BCS. The latest event, at 1.4 BY, a high grade contact metamorphism related to the protracted intrusion of the Laramie Anorthosite Complex (LAC) at approximately 3 kb, resulted in high temperatures (locally >> 700°C) and partial melting of metapelites within 2 km of the LAC intrusive contact.

Contact metamorphic mineral assemblages in the BCS record both increasing temperatures and decreasing $X(H_2O)$ towards the LAC contact. Five isograds determined using metapelites are located within 3 km of the contact whereas one mapped isograd is based on metacarbonate equilibria. An isobaric T-$X(H_2O)$ diagram (Grant, 1985) shows BCS metapelitic equilibria could exist nearly isothermally at sub-solidus temperatures at varying $X(H_2O)$. However, textural evidence of partial melting in metapelitic compositions increases toward the intrusive contact. Leucosomes, restites, lathe-shaped

plagioclase, orthopyroxene overgrowths, euhedral cordierite and quartz, bimodal biotite grain size and fabric, and oikocrystic K-feldspar and quartz are all consistent with the presence of melt. Phase equilibria and textural evidence (especially inclusion relations and igneous morphology) are consistent with melt-forming reactions emanating from a single isobarically invariant point. Two schematic isobaric liquidus diagrams are presented, one for $X(H_2O)$ lower and one for $X(H_2O)$ higher than the value for the invariant point.

In the Bluegrass Creek suite both the temperature and the composition of the coexisting vapor phase are important variables for melting relations. Metapelitic compositions melting at different $X(H_2O)$ results in different melting relations. These relations provide important clues to the process of anatexis at moderate crustal levels. Although garnet-bearing restites formed by incongruent melting of metapelites probably reflect a lower $X(H_2O)$ and/or higher temperature than required to produce orthopyroxene-rich restites, it appears that eutectic crystallization of orthopyroxene requires lower $X(H_2O)$ than does garnet. The vapor absent melting reaction (at the invariant point) is potentially the most important based on the scarcity of orthopyroxene coexisting with garnet in the BCS.

TABLE OF CONTENTS

LIST OF FIGURES

Figure

Figure

CHAPTER 1: INTRODUCTION

Problem

The purpose of this thesis is to describe and interpret the contact metamorphic effects, including partial melting, within the contact aureole along the northern border of the Proterozoic Laramie Anorthosite Complex. This thesis concentrates primarily on the pelitic compositions since they display the most variability mineralogically and texturally, but also because these compositions begin to melt at relatively low temperatures.

The objectives of this study are to: (1) map and sample in detail the rocks of the Bluegrass Creek Suite, (2) determine the mineral assemblages present and deduce metamorphic facies, (3) apply knowledge of mineral equilibria in conjunction with macroscopic and microscopic textural evidence to differentiate the relict regional metamorphic textures from those produced during the contact event, 4) determine the textures and mineralogies which result from partial melting and subsequent crystallization of the derived silicate melts.

General Statement

The study area was chosen because: (1) the rocks have not undergone further metamorphism since the contact metamorphic event, (2) the area provides a wide variety of lithologies, including pelites, which melt at relatively low temperatures, (3) the rocks are well exposed and readily accessible.

This thesis first provides a geologic background for the area. The observations made during this study are then presented. Finally, interpretation of the metamorphic history in the study area, including partial melting is discussed.

Location and Access

The study area lies along the northern contact of an intrusive hornblende syenite (a late phase of the Laramie Anorthosite Complex) in the Central Laramie Mountains (Figure 1.1). The field area straddles the border between Albany and Platte counties and encompasses about 6 km^2 within sections 4, 5, 6, 7, 8, and 9 of T.22N, R.70W (Plate 1). The rocks of the Bluegrass Creek Suite are readily accessible via Tunnel Road which runs west from State Route 34 (Figure 1.2). In the study area, the Bluegrass Creek Suite lies south of Squaw Mountain and north of Tunnel Road and outcrops in rolling hills utilized for grazing and hunting. The rocks are well exposed, with approximately 30% outcrop.

Methods of Study

Six weeks of detailed mapping (1:12000) during July and August of 1986 provided the foundation for this research. Sampling covered all units, but pelitic compositions make up

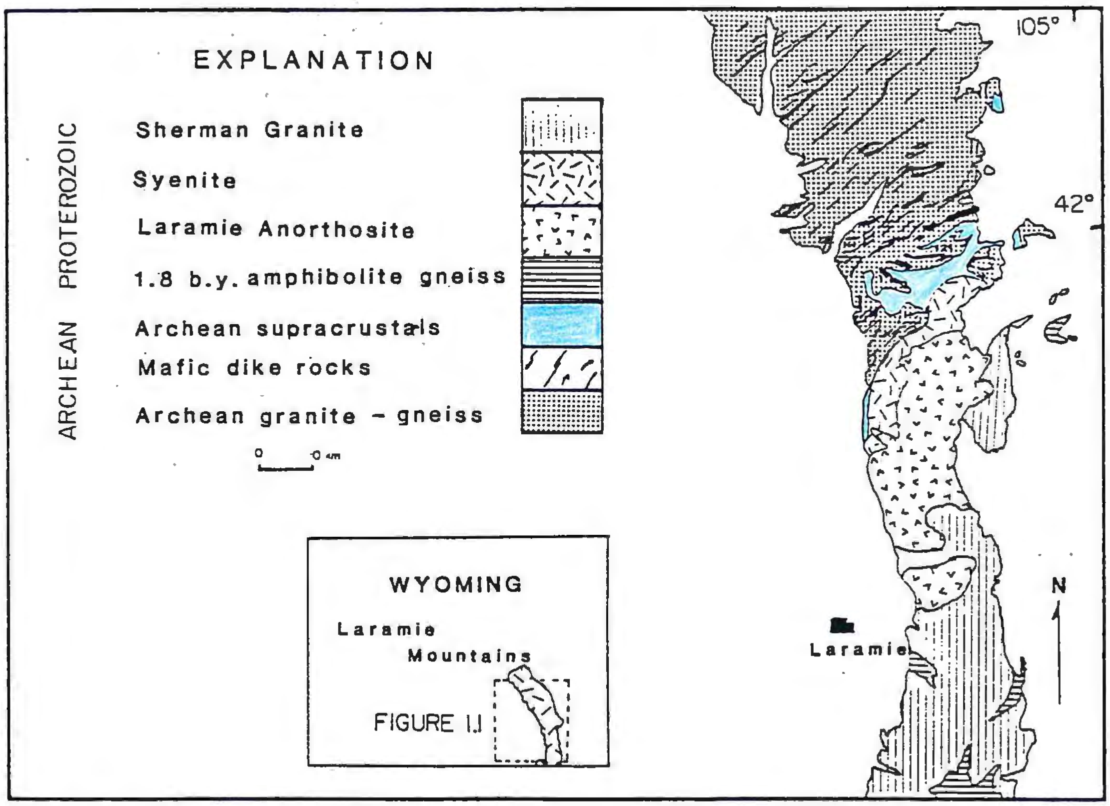

Fig. 1.1. Distribution of Precambrian rocks of the Laramie Mountains, south-eastern Wyoming, after Graff et.al., 1982. Unornamented areas are Phanerozoic rocks.

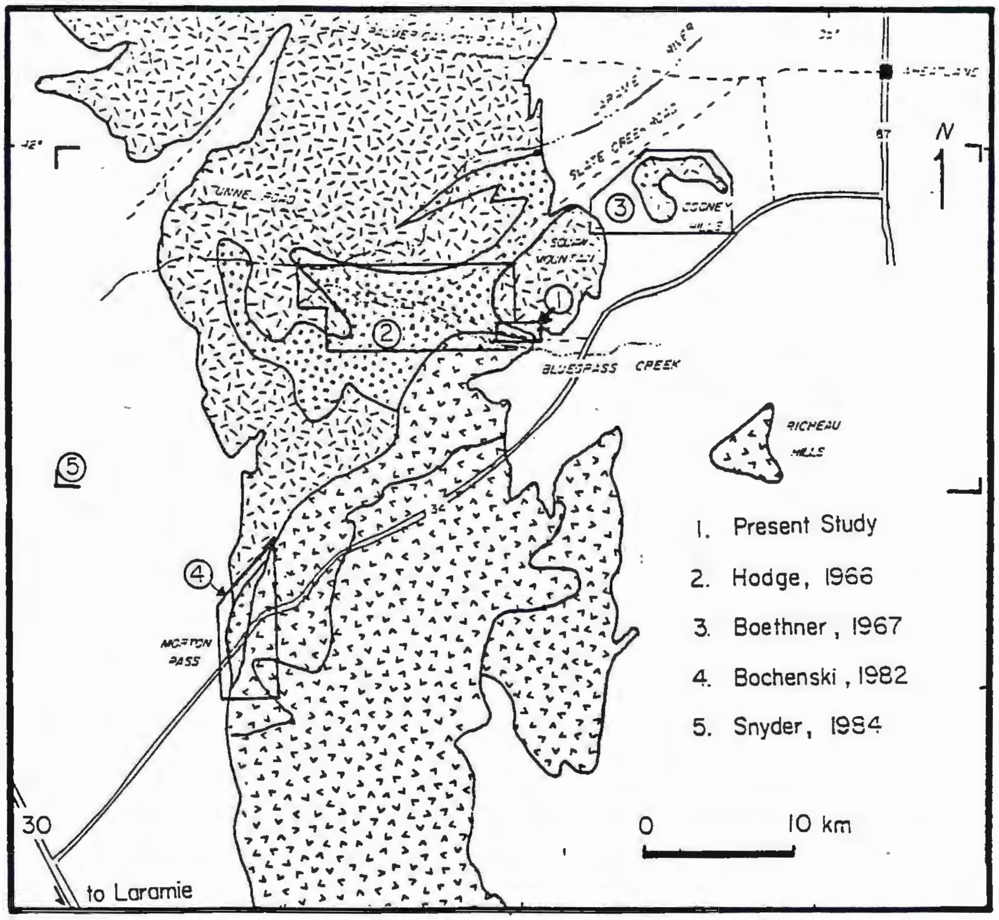

Fig. 1.2. Previous work in the Central Laramie Mountains. Dashed pattern is Archean granite gneiss terrain. Double-dashed pattern is Archean supracrustal rocks. V pattern is Proterozoic intrusives. Phanerozoic rocks unornamented.

the majority of the 175 specimens collected. 125 samples were chosen for thin section analysis. Using grain to grain contact in thin section as a conservative criterion for equilibrium, the probable equilibrium assemblages were determined. Mineral compositions were estimated using petrographic microscope and known mineral compositions from similar rocks in the Morton Pass area as determined by Grant (1985). Published data were used for comparison to determine approximate metamorphic conditions.

Previous Investigations

The early work in the Laramie Mountains concentrated almost exclusively on the igneous rocks of the Laramie Anorthosite Complex. The earliest work by Darton et al. (1910) presented an overview of the anorthosite complex. Fowler (1930) described the petrography of the anorthosite whereas Devore (1948) and Newhouse and Hagner (1945, 1947) proposed a metasomatic origin for the complex. Klugman (1960) reverted to an igneous origin for the complex.

Hodge (1965) presented the structure and metamorphism of the Precambrian rocks of the Bluegrass Creek area, focusing primarily on the 2.6 b.y. metamorphism. Bothner (1967) described the petrology of the Precambrian rocks of the Cooney Hills, and Bochenski (1982) discussed the contact metamorphism associated with the intrusion of the Laramie Anorthosite Complex at the Morton Pass area. Snyder (1984) described the Precambrian rocks of much of the Central Laramie Mountains and his reconnaissance scale mapping provided the framework for mapping done in this study.

Continuing studies include the detailed mapping of and work on the origin and mode of emplacement of the Laramie Anorthosite Complex by B.R. Frost and D.H. Lindsley. Contact metamorphic effects and models for partial melting in the aureole were presented by Grant (1985a) and by Grant and Frost, (1986). A detailed investigation of contact metamorphism and partial melting in the Morton Pass area by Grant and Frost is in press.

Support for Partial-Melting

The effects attributable to the process of partial melting are of primary interest in this thesis. This section attempts to approximate the minimum temperature attained near the contact of the intrusion of the Laramie Anorthosite Complex in the study area.

A first approximation of temperatures achieved in the contact aureole can be estimated utilizing a simple model described by Jaeger (1964). The first assumption to be made is that the Bluegrass Creek Suite (BCS) was intruded by the Laramie Anorthosite Complex (LAC) at pressures of about 3.0 kb (approximately 10 km). This assumption seems valid based on the work done at Morton Pass by Grant and Frost (in press). Using a low geothermal gradient of $25^{\circ}C/km$, a calculated minimum temperature for the BCS prior to intrusion is $250^\circ C$.

Other assumptions inherent to this model (which appear to be justifiable for the simple model being considered) are that the contact is planar, the rocks of the BCS have roughly the same thermal conductivity as the intrusives, and that the rocks are essentially dry (earlier amphibolite facies metamorphism would have driven off much of the water). There are other assumptions to be made which should have smaller effects (see Jaeger, 1964) which are not accounted for here.

For this oversimplified case the intrusion of the anorthositic phases of the LAC will be assumed to be instantaneous. The temperatures for emplacement of the anorthositic rocks are roughly $1100^\circ C$ (B.R. Frost, pers. comm., 1986). Following Jaeger (1964, 1968) but ignoring any latent heat of crystallization, the temperature at the contact (T_c) will be the original temperature of the country rock (T_o) plus one half of the temperature difference between the country rock (T_o) and the initial temperature of the anorthosite at the time of intrusion (T_i):

$$T_o + [(T_i - T_o)/ 2] = T_c \qquad (1)$$

$$250^\circ C + [(1100^\circ C - 250^\circ C)/ 2] = 675^\circ C$$

This calculation yields a temperature of $675^\circ C$ for the contact after the intrusion of the anorthositic phases.

Since the anorthositic phases probably were intruded as crystal rich liquids (Frost, pers. comm. 1986), ignoring latent heat of crystallization may be a valid assumption. However, for the second phase of intrusions (the syenites), ignoring the latent heat of crystallization would lead to the calculation of a minimum temperature.

The radiometric dating of all the phases of the Laramie Anorthosite Complex cluster around 1.4 b.y. (Graf et al., 1982). However, the time elapsed between the intrusion of the main anorthosite body, which is 40-50 km long and 10-15 km wide, and the smaller volumes of syenitic magmas (figure 1.1) cannot be resolved with present analytical techniques. The anorthosite appears to have been cool enough to react brittly where it is crosscut by the syenite. This is not surprising if the anorthosite intruded in a partially crystallized condition (e.g. less than 50% interstitial silicate liquid). Another potential indication for a close temporal relation is the preponderance of mixed dikes which may represent the immiscible mingling of two or more chemically distinct magmas (Stafford & Lindsley, 1986).

Since the difference in ages of the anorthosite and the syenite, as determined radiometrically (Snyder, 1985) is nil, (though errors may be significant) and considering the size of the anorthositic body, it is likely that the Bluegrass Creek Suite was intruded by the Red Mountain Syenite (RMS) before significant cooling. The RMS was intruded at approximately 900°C (Anderson & Frost, 1986). Similar calculations (again using equation 1 and ignoring the additive effect of the latent heat of crystallization) lead to temperatures for the country rock (BCS) at the contact of 787.5°C.

$$675^{\circ}C + [(900^{\circ}C - 675^{\circ}C)/ 2] = 787.5^{\circ}C$$

If the effects of latent heat of crystallization are taken into account, they could easily add 30°C or more to this estimate. These calculations also ignore the effects of sills of the Red Mountain Syenite which interfinger with the Bluegrass Creek Suite subparallel to the contact which could only have had an additive effect on the temperature profile through the area.

At pressures of 3.0 kb and temperatures of 785°C, pelitic compositions, even if they are essentially dry (intergranular H_2O is absent, micas constitute the major source of H_2O), are well above the beginning of melting. These calculations suggest conditions were favorable for the production of pelitic migmatites.

CHAPTER 2: GEOLOGIC HISTORY

In order to place the Bluegrass Creek Suite in a geologic setting, this chapter presents the pertinent information concerning the development of the rocks of the Central Laramie Mountains and some interpretations of the tectonic setting in which these rocks formed. The interpretation of the stratigraphy is followed by a discussion of metamorphism, uplift, and exposure.

Stratigraphy

The stratigraphy in the study area is especially complex due to the local concentration of sills associated with the Red Mountain Syenite. However, a few miles to the west in the Slate Creek belt (figure 1.2), the stratigraphy is fairly well known and is grossly consistent with the rocks in the present study area (Hodge, 1966; Graf et al, 1982; Snyder, 1984). Relations between the supracrustals and the granitic gneisses (also dated at 2.6 b.y.) suggest they may have been deposited directly on the gneisses, but locally, intrusive relations are indicated (Snyder, 1984). A U-Pb zircon age of approximately 2.6 b.y. for the rocks of the Bluegrass Creek Suite was obtained from a rhyolite flow which occurs within the stratigraphy in the Slate Creek Belt to the west of the study area (K.R. Ludwig, pers. comm., 1985).

The stratigraphy of the Bluegrass Creek Suite can be broken into two major lithologic units (Snyder, 1984). The lower unit consists dominantly of amphibolite with minor marbles. The amphibolites are generally well-layered and have been interpreted by Snyder (1984) to be water-laid basaltic ash.

The lower unit is overlain by a highly variable sequence of metasediments; Pelitic and calcareous schists and gneisses are the most abundant rock types, but quartzite, amphibolite, and meta-conglomerate are locally significant. Banded iron formation is reported in the Slate Creek belt (Graf et al., 1982) but no convincing iron formation was found in the study area.

These units have been interpreted as shelf-type deposits along the southern edge of the Archean Wyoming craton (Graf et al, 1982) whereas Snyder (1984) suggested a back-arc environment for deposition of these units. Duebendorfer and Houston (1987) have interpreted the supracrustal sequence to be the result of miogeoclinal deposition.

Contact Relations

In the central Laramie Mountains, the Archean supracrustal rocks have conformable sedimentary contacts with Archean gneisses and granites locally (Grant, J.A., pers. comm., 1986) whereas some locations have intrusive or faulted contacts (e.g. present study), suggesting two distinct ages of Archean granites.

Amphibolite dikes cut the Archean granites and gneisses throughout the Laramie Mountains. In the present study, the relationship between the amphibolite dikes and the contact between the granite and the supracrustals was not determined.

In the study area, two distinct types of contacts between Archean supracrustal rocks and the Archean Squaw Mountain Granite are present. The western half of the contact appears to be intrusive, while the eastern half is composed of highly sheared rocks (now blastomylonites) and appears to be a fault contact.

Regional Metamorphism

The rocks of the BCS were folded and metamorphosed to amphibolite facies during a regional metamorphism dated at 2.6 b.y. (Graf, et al., 1982). Inclusions of BCS in the Squaw Mountain granite are found near the contact and indicate that the granite is, at least in part, younger than the BCS. Graff et al. (1982) suggests the Squaw Mountain granite was intruded during a significant doming event. The Squaw Mountain granite is a high-potassium granite and is either syn- or post- 2.6 b.y. regional metamorphism.

In the regionally metamorphosed pelitic rocks, the common assemblage is quartz-plagioclase-aluminosilicate-biotite-garnet-staurolite (Hodge, 1966; Grant & Frost, 1986). The aluminosilicates present in the regional assemblage are kyanite and sillimanite and thus establish pressures above the aluminosilicate triple point (figure 2.1). The sillimanite occurs as fibrolite foliation and is interpreted to be late, replacing a muscovite foliation through the reaction quartz + muscovite + staurolite = sillimanite + biotite + garnet (figure 2.1).

Grant and Frost, 1986, using the biotite - garnet geothermometer of Ferry and Spear (1981), reported preliminary data from the cores of zoned garnets from the regional event suggesting temperatures of around 600°C. Using the garnet-aluminosilicate-quartz geobarometry of Haselton and Newton (1981) they estimated pressures of at least 6 kilobars. These cores were interpreted by Grant and Frost (1986) to have equilibrated near the culmination of the regional metamorphic event (2.6 b.y.). They also reported that the garnet rims are high in iron relative to the cores and suggested subsequent growth or reequilibration at lower pressures and temperatures.

Between 1.8 and 1.6 b.y., movement along the Mullen Creek - Nash Fork shear zone (Cheyenne Belt, Figure 2.2) exceeded 10 km vertically and perhaps hundreds of km horizontally (Hills & Houston, 1979) . This zone is interpreted to be a suture which resulted from the collision of an Archean Wyoming province with a Proterozoic island arc (Duebendorfer & Houston, 1987). Evidence of this shear zone extends from

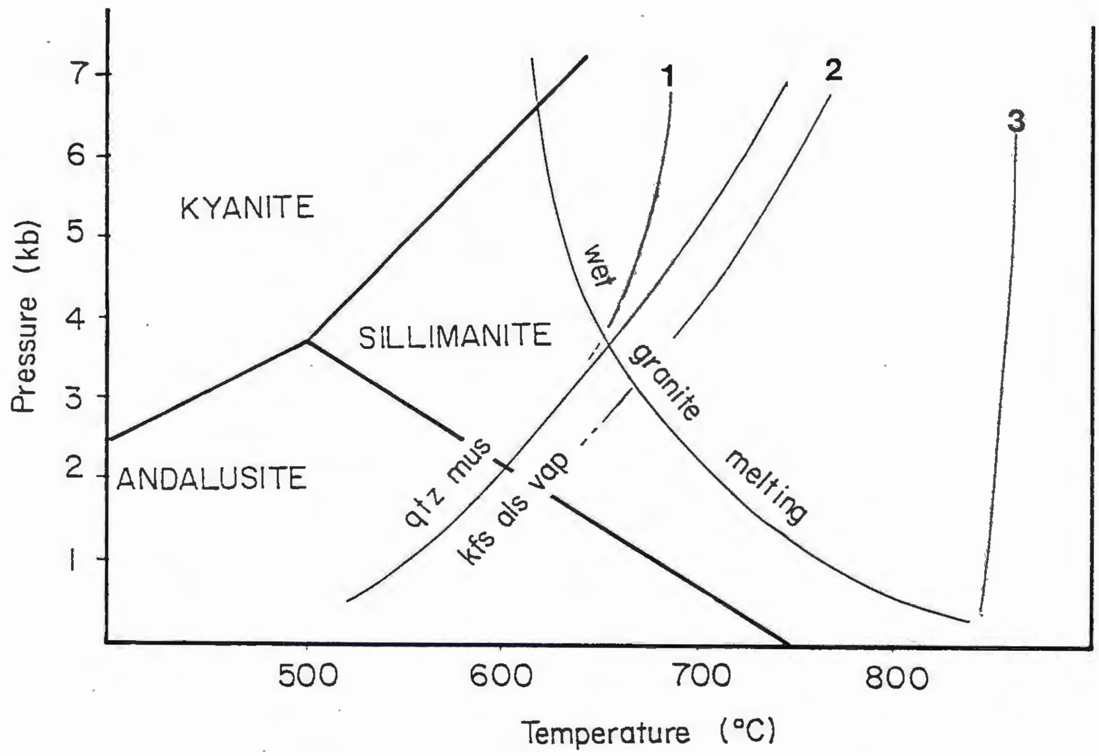

Fig. 2.1. Pressure-temperature diagram showing important reactions in the Bluegrass Creek suite. Reaction 1 is Qtz + Mus + Sta = Bio + Sil + Gar + vap taken from Richardson, 1968. Reaction 2, Mus = Kfs + Corundum + vap, and the breakdown of Qtz-Mus are taken from Chaterjee and Johannes, 1974. Reaction 3, phlogopite + quartz = sanidine + enstatite + liquid is from Bohlen et al, 1983. The Aluminosilicate triple point is from Holdaway, 1971.

NE Utah through southern Wyoming. Many workers, including Duebendorfer and Houston (1987) suggest it may extend further east through the Richeau Hills (Figure 1.2). No evidence for this structure has been reported in the Laramie Range.

Contact Metamorphism

At about 1.4 b.y. the Laramie Anorthosite Complex (LAC) intruded the Bluegrass Creek Suite. The LAC is a multiple intrusion with rock types ranging from anorthosite to granite (Graff et al., 1982). The main anorthositic body is about 40 km long and 10 km wide and is composed of rocks ranging from gabbro to anorthosite with local concentrations of oxides. Two lithologically distinct syenites are younger than the anorthositic phases and rim the anorthosite to the north (Figure 2.3). The Sybille syenite (a pyroxene syenite) cuts and includes anorthositic phases. The Red Mountain syenite (a hornblende syenite) cross cuts the Sybille and therefore must be later than the Sybille syenite (I.C. Anderson, pers. comm.).

On the basis of contact metamorphic assemblages in the Morton Pass area approximately 45 km southwest of the study area, the pressure at emplacement was 3.0 ± 0.5 kb (Grant,1985a; Grant & Frost, in press). The anorthosite yields a crystallization temperature of approximately 1100°C, the Sybille syenite about 1020°C (Fuhrman et al., in press), and the Red Mountain syenite intruded at about 900°C (Anderson & Frost, 1986).

The intrusion of the Red Mountain Syenite resulted in the emplacement of many sills which are mineralogically similar to (and probably cogenetic with) the RMS but contain significantly more modal quartz (i.e. they are granitic). No geothermometry or geobarometry has been done on the sills.

The final phase of the LAC may be the Sherman Granite, which also is dated at 1.4 b.y. (though anomalously old ages have been determined from assimilated zircons, cross cutting relations indicate the Sherman Granite is younger)(Snyder, 1984). This unit does not occur in the field area, but does rim the anorthosite on the east and south, and forms an intrusion of batholithic proportions, from the southern contact of the main anorthosite well into northern Colorado. The genetic relationship between the Sherman Granite and the rest of the LAC is not well constrained.

Since the intrusion of this extremely large igneous complex during Middle Proterozoic time, the rocks of the area have not been intruded or metamorphosed. By Pennsylvanian time they had been uplifted and exposed as part of the ancestral Rocky Mountains, and are now unconformably overlain to the west by the Pennsylvanian Casper formation. Laramide (80-60 Ma) uplift accounts for their present elevation (4000-7000 feet above mean sea level). The valley fill to the east and west consists of Tertiary gravels and Quaternary alluvium. Evidence for glaciation is absent.

CHAPTER 3: STRUCTURE

2.6 B.Y. Regional Event

The large scale structural features in the supracrustal rocks of the central Laramie Mountains result from at least two deformations of an originally horizontal heterogeneous layered sedimentary pile (Hodge, 1966). Recent work by Snyder (1984), particularly north and west of the present study area supports this interpretation.

Hodge (1965) delineated a first deformation in which the rocks were folded into open synclines and anticlines. The gneisses in the BCS acquired their initial fabric (most likely a mica-rich foliation) during this first deformation. The second deformation, characterized by isoclinal folding with axial planes trending north and dipping moderately to the east may include some large scale nappes, though their existence is not yet proved.

These Archean supracrustal rocks were dubbed the "Elmer's Rock Greenstone Belt" by Graff et al. (1982), primarily based on structural and stratigraphic similarities with "classic" greenstone belts. Structural similarities observed in the BCS include vertical to subvertical synformal and antiformal supracrustal rocks intruded by syntectonic and/or post-tectonic granites. The stratigraphy of the BCS is typical of the upper part of classic greenstone belts, with amphibolites lying stratigraphically lower in the pile than pelites, quartzites and marbles (topping directions from pillow lavas). Small ultramafic bodies outcrop and are chemically similar to lower greenstone belt komatiites. Finally, the whole sequence is intruded by syn- to post-tectonic granites (e.g. Squaw Mountain).

1.4 B.Y. Intrusion of the Laramie Anorthosite Complex

It is clear from the maps of Hodge (1965) and those of Snyder (1985) that the structural elements in the Bluegrass Creek Suite within 1 km of the contact with the Red Mountain Syenite have been modified by the intrusion of the complex. Previously existing foliations, folds, and linear features were rotated sub-parallel to the intrusive contact of the Red Mountain Syenite (see Hodge, 1965). In the eastern part of the field area, structural trends are roughly NW-SE; in the central part, the foliation swings to E-W, and in the west becomes NE-SW (Plate 1). These features suggest forceful intrusion. Since the layering in the rocks is sub-vertical, and foliations and fold axes are sub-parallel to layering, maps showing lithologic variation also illustrate the major structural elements fairly accurately. Lithologic layering is very discontinuous and, even though well exposed, is rarely traceable along strike for more than a kilometer, due in part to the network of sills of the RMS.

Folds with wavelengths of greater than 10 meters were observed only where quartzites were prominent, probably due to their different competency with respect to other supracrustal lithologies. Small scale folds, which may be parasitic, are present in all the supracrustals, but are especially conspicuous in K-feldspar-cordierite gneisses in which relict bedding and/or metamorphic differentiation has created an easily identifiable layering within the unit.

Fold axes characteristically lie subparallel to the lithologic layering and plunge moderately to steeply both to the west and east. Locally, a foliation is defined within the K-feldspar-cordierite gneisses which is at a moderate angle (20-40°) to the compositional layering (figure 3.1). This foliation is manifested in darker, oriented elongate blebs of cordierite-rich material surrounded by lighter colored thin leucocratic zones. Mineral lineations are rare, developed only in areas of highest strain which are associated with faults.

Evidence of significant faulting is found along the NE border of the supracrustal units where the Bluegrass Creek Suite is in contact with the Squaw Mountain Granite (plate 1). The Squaw Mountain granite is typically a slightly foliated porphyritic biotite granite with megacrysts of K-feldspar up to 6 cm across. Less than 200 m. from the contact with the Bluegrass Creek Suite, the granite grades into an augen gneiss with progressive rounding and mechanical destruction of the large orthoclase megacrysts towards the contact. The most highly deformed Squaw Mountain granite (a

Fig. 3.1. Segregation in K-feldspar-cordierite gneiss. Light areas are dominated by quartz and K-feldspar. Dark areas contain abundant cordierite. Sample locality 20.

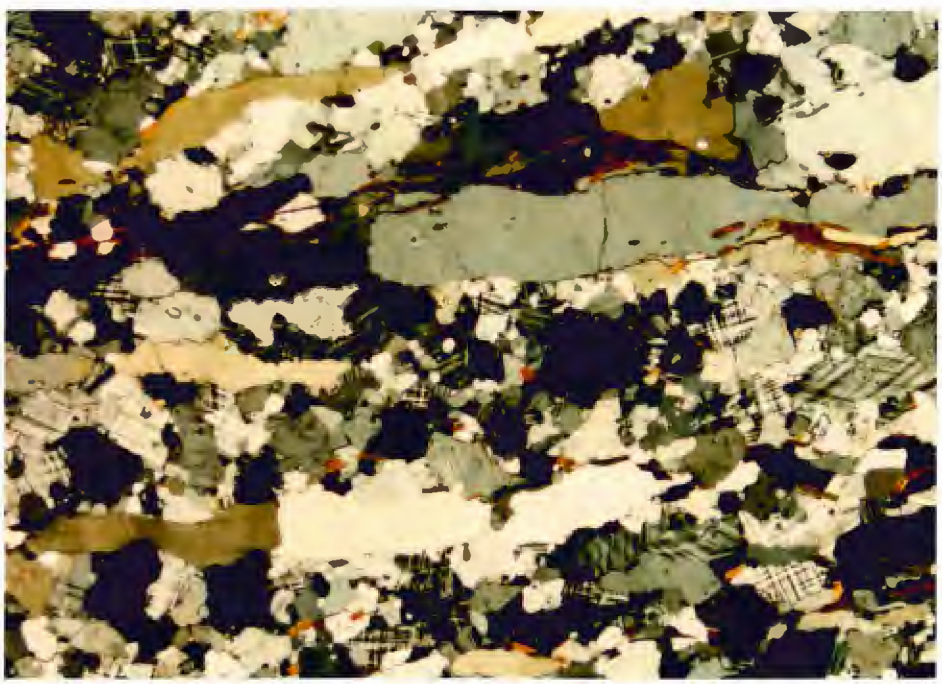

Fig. 3.2. Photomicrograph of deformed Squaw Mountain granite displaying blastomylonitic texture. Sample locality SR-5. Crossed polars. Photo is 9 mm. across.

blastomylonite) has elongate blebs of quartz parallel to foliation (Figure 3.2). These quartz "ribbons" are essentially strain free, indicating significant static recrystallization, possibly during the intrusion of the Laramie Anorthosite Complex, less than 1 km away.

Adjacent to the zone of intense shear, the amphibolites of the Bluegrass Creek Suite show elongate quartz boudins parallel to foliation. These boudins range in scale from the microscopic (within the amphibolites) (figure 3.3) to 10 cm thick or more where quartz veins are interlayered with the amphibolite. In amphibolites in the northwest corner of the field area (plate 1), garnets (up to several cm across) contain inclusion trails which suggest rotation during growth.

Agmatite (a brecciated amphibolitic gneiss cut by granitic veins and dikes of granitic material) is well exposed in a cliff face north of the Huston ranch just south of the highly deformed Squaw Mountain granite. The shape of the blocks of amphibolite gneiss (typically meters to tens of meters in diameter) change from roughly equant angular blocks to elongate lenses from south to north. The appearance of the rock changes drastically from an injected breccia to a highly deformed gneiss. Due to the nature of the contact, the timing of the agmatization remains ambiguous.

Another fault (possibly very late) may be the source of a unique rock composed of brecciated tan chert with minor

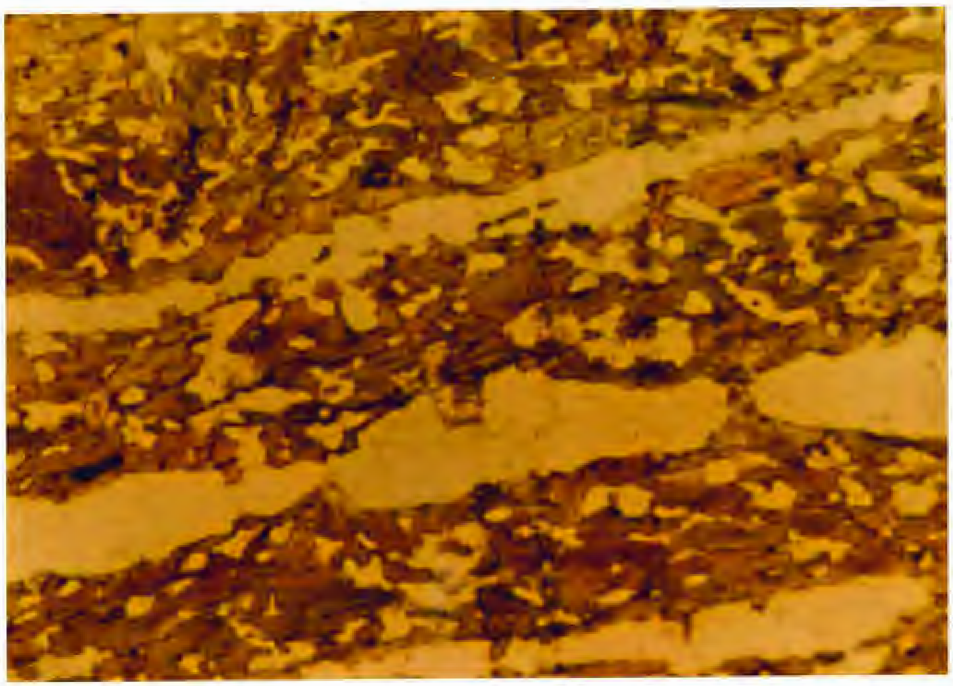

Fig. 3.3. Photomicrograph of sheared amphibolite with micro-boudins of quartz in a hornblende and quartz-rich matrix. Sample locality 33. Plane polarized light. Photo is 3.5 mm across.

amounts of sulfide minerals and books of purple mica (lepidolite?) which is now cemented by white botryoidal chalcedony. Samples were found concentrated in the float near the center of the study area (sample locality F1, plate 2)

The mode of emplacement of the Laramie Anorthosite Complex is still under investigation. The anorthosite was probably significantly crystallized before emplacement (a cumulate) and probably rose diapirically. Proposed emplacement models include diapiric ascent and/or forceful intrusion with variable amounts of block stoping.

CHAPTER 4: LITHOLOGIC DESCRIPTIONS

This chapter is largely descriptive, presenting the gross characteristics of the mapped units. Mineral species are discussed for the pelitic units as these rocks show the most variability. Equilibrium assemblages and data pertinent to the metamorphism are deferred to the next chapter.

SUPRACRUSTAL UNITS

AMPHIBOLITE

Green to black, medium to coarse-grained, massive to well-layered amphibolite is common. Local varieties include a garnetiferous "turkey-track" amphibolite, with sprays of hornblende up to 15 cm long (figure 4.1), and a garnetiferous unit with subhedral garnets up to 8 cm across (figure 4.2). Well-layered units are interlayered with massive units, which are interpreted by Snyder (1984) as sills of andesitic basalt intrusive into water-laid basaltic ash. The amphibolite unit is thickest in the NW corner of the study area where it is in excess of 100 meters thick (plate 1). In areas of high strain (shear zones), quartz occurs as elongate bands parallel to foliation and as boudinaged veins. The amphibolite commonly consists of hornblende, plagioclase, quartz and opaques $\pm$ biotite, $\pm$ cummingtonite, $\pm$ clinopyroxene, $\pm$ sericite, $\pm$ chlorite.

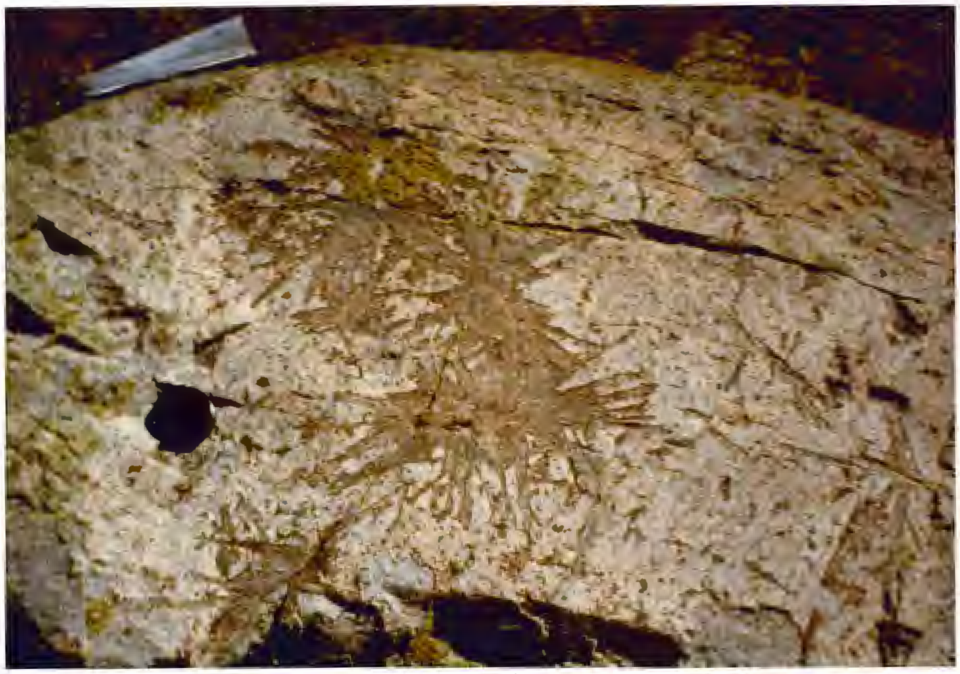

Fig. 4.1. Turkey track amphibolite. Splays of amphibole lie parallel to foliation. Lens cap for scale. Sample locality MP-9.

Fig. 4.2. Garnitiferous amphibolite. Garnets locally exceed 4 cm in diameter. Lens cap for scale. Sample locality MP-9

MARBLE AND CALC-SILICATE ROCKS

White to grey, medium to coarse-grained, massive to well-foliated marbles predominate. Where calc-silicates and/or phlogopite are abundant, layering and crude preferred grain orientation are common, yielding layered gneissic marbles. Grey-green tremolite, yellow-orange forsterite, and dark green diopside are the major silicates present accompanying the calcite. Phlogopite, graphite, spinel, scapolite, and sphene are also abundant locally. Alteration of olivine to serpentine is extensive.

Varieties of carbonate-rich rocks include ophicalcite and a very well-laminated rock (figure 4.3) which occurs locally immediately adjacent to sills of the RMS. This rock consists of alternating white and green to blue- grey laminae. The white layers are almost pure calcite whereas the darker layers are serpentine-rich. Originally, the geometry of this compositional layering lead workers to propose a biogenic origin (stromatolitic), however, compositional layering cross-cuts the lithologic layering and it is clearly a contact-metamorphic phenomenon related to diffusionally controlled processes.

The calc-silicate rocks are green to dark brown, medium to coarse-grained massive rocks which occur as pods and lenses within the marbles as well as along the contact with other lithologies. The mineralogy is highly variable, and consists of various combinations of tremolite, hornblende,

Fig. 4.3. Hand samples of calcite - serpentine rock (ophicalcite). Upper left sample is cut surface. Penny for scale.

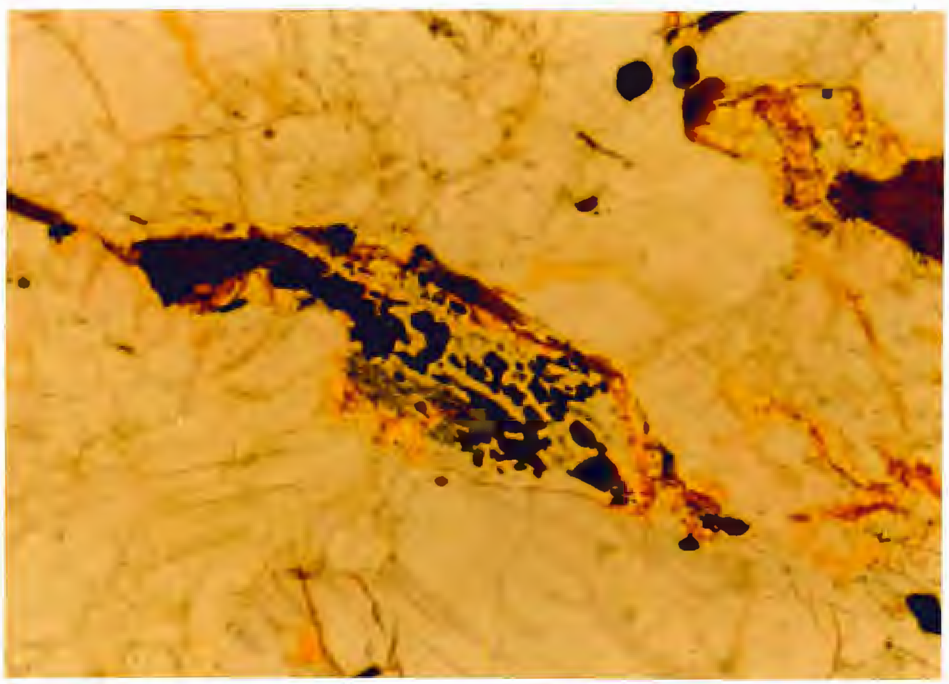

Fig. 4.4. Photomicrograph showing aluminous knot. Sillimanite needles and green spinel are encased in cordierite. The matrix is K-feldspar, biotite, and quartz. Sample 28.2. Plane light. Photo is 3.5 mm across.

plagioclase, biotite, diopside, calcite, sphene, graphite, scapolite, and clinozoisite.

QUARTZ-FELDSPAR-BIOTITE GNEISS

This highly variable unit grades from a massive quartzofeldspathic biotite gneiss to banded migmatitic gneiss. However, these rocks are commonly closely associated and were mapped as a single unit.

Quartzofeldspathic biotite gneiss is generally tan weathering, but grey on the fresh surface. Commonly well foliated and medium-grained, it contains abundant quartz, sub-equal proportions of K-feldspar and plagioclase, and less than 10% biotite. The unit typically has significant zircon, opaque oxides, and traces of muscovite and chlorite.

The banded migmatitic gneiss consists of leucocratic layers and lenses of coarse-grained quartz, K-feldspar, plagioclase, biotite, $\pm$ garnet, and dark, biotite-rich layers and lenses which contain plagioclase, K-feldspar, opaques, $\pm$ quartz, $\pm$ garnet, $\pm$ muscovite, $\pm$ chlorite. Layers are typically 10 to 50 cm. wide, but locally are more than a meter. The proportion of leucocratic material to biotite-rich material is generally less than 1:1.

QUARTZITE

Light blue to white, medium- to coarse-grained quartzite displays a range in bedding thickness from 3 cm to a few meters. Quartzite is locally abundant (e.g. sample locality SM20, Plate 2). Quartz makes up over 90% of the rock, the remainder being K-feldspar, biotite, sericite and opaques. The quartzites are typically thin (< 1 meter thick) and usually found interlayered with the K-feldspar-cordierite gneiss.

K-FELDSPAR-CORDIERITE GNEISS

Dark blue-black to buff, fine- to coarse-grained K-feldspar-cordierite gneiss commonly contains blebs, lenses, pods, layers, and veinlets of rusty weathering leucocratic material (figure 3.1). The subtle blue hue can be directly correlated to the presence of cordierite. The major mineralogy of the bulk of the rock is K-feldspar, cordierite, quartz, biotite, $\pm$ plagioclase, $\pm$ sillimanite (prismatic and fibrolitic), $\pm$ andalusite, $\pm$ garnet, $\pm$ hercynite, $\pm$ corundum, $\pm$ orthopyroxene, $\pm$ muscovite, $\pm$ opaques, $\pm$ rutile, $\pm$ graphite, $\pm$ tourmaline, $\pm$ zircon, $\pm$ chlorite. It grades into biotite gneiss with increasing biotite, quartz and feldspar, and decreasing cordierite.

K-feldspar is principally microcline and occurs either as anhedral to subhedral grains, or as large oikocrysts with inclusions of quartz and cordierite. K-feldspar is especially abundant in the coarser leucocratic material.

Cordierite occurs as anhedral blebs in K-feldspar oikocrysts, as mosaics surrounding aluminosilicate and/or hercynite (figure 4.4), and as subhedral to euhedral crystals (e.g. in rocks containing orthopyroxene), commonly with abundant inclusions and pleochroic halos around zircon. Cordierite is altered to pinnite along grain boundaries.

Anhedral quartz is ubiquitous, associated with and included within biotite, K-feldspar, plagioclase, and garnet. It also is found as oikocrysts (in poikilitic orthopyroxene-bearing rocks) with inclusions of feldspar, cordierite, and orthopyroxene.

Biotite is found in a variety of assemblages and textures. It defines the foliation along with acicular and fibrolitic sillimanite; Large masses, books, and platy crystals occur in leucocratic layers. Orthopyroxene bearing rocks contain skeletal, corroded grains of biotite.

Plagioclase occurs in anhedral to nearly euhedral crystals and is commonly associated with quartz, biotite, garnet, and K-feldspar. It also occurs as exsolved blebs (or cores) in and as rims around microcline grains. Plagioclase rarely forms elongate laths within a mosaic of K-feldspar, quartz, and cordierite (figure 4.5).

Sillimanite is the most abundant aluminosilicate polymorph. Occurring as needles, prisms, and fibrolitic masses (figure 4.6) it is commonly associated with hercynite, biotite, cordierite, and garnet. Locally sillimanite is surrounded by mosaics of fine grained cordierite and K-feldspar.

Andalusite crystals occur as colorless to pale rose pleochroic anhedral grains and poikiloblasts. Samples

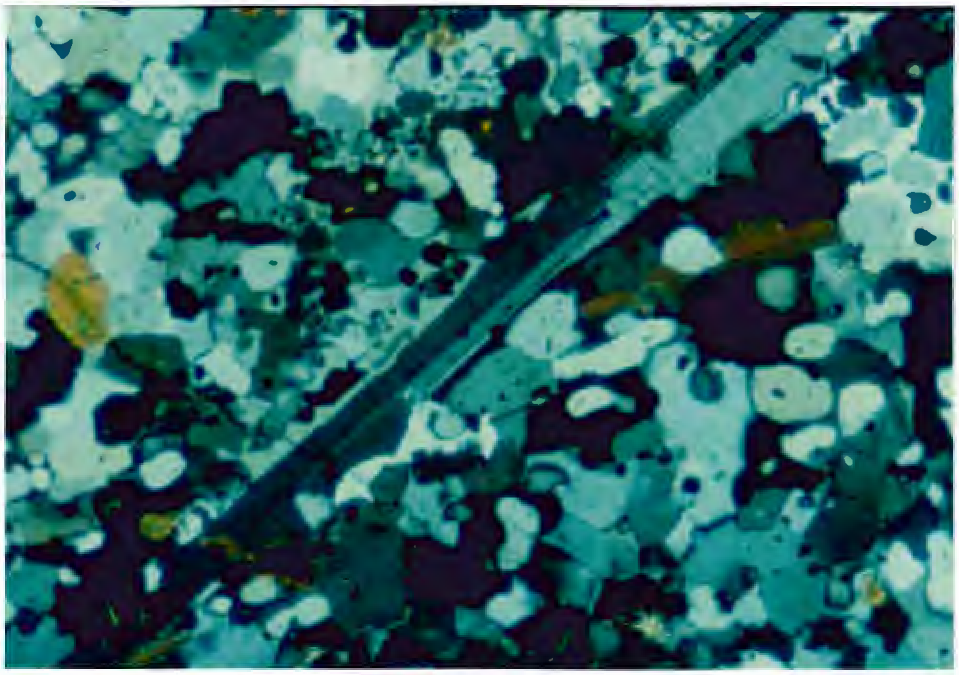

Fig. 4.5. Photomicrograph of "igneous" plagioclase enclosed in matrix of quartz, K-feldspar, cordierite and biotite. Sample GMP30-1 (from Grant & Frost, 1986) Crossed polars. Photo is 3.5 mm across.

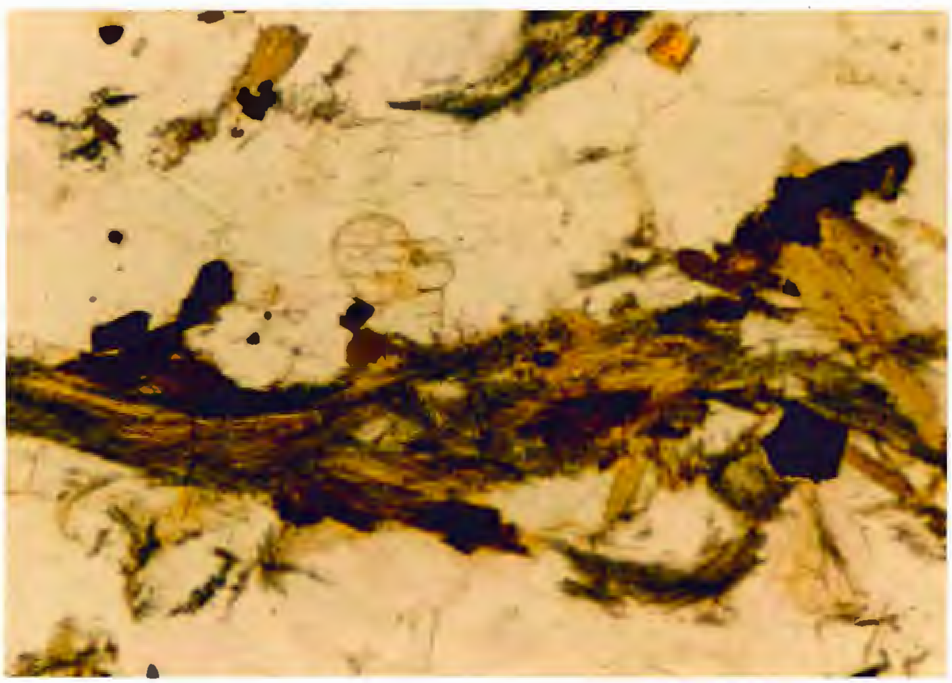

Fig. 4.6. Photomicrograph of contorted fibrolite masses. Cordierite crystals are altered along rims to pinnite (yellow). The matrix is biotite, quartz, and K-feldspar. Sample 20-6. Plane light. Sample is 3.5 mm across.

bearing andalusite are restricted to rocks containing abundant sillimanite, biotite, and hercynite.

Garnets are common in at least two distinct situations. One occurrence is as porphyroblasts in biotite-rich pelites. The other common occurrence is in leucocratic layers and lenses (figure 4.7). The garnets in the biotite rich rocks are primarily subhedral to euhedral porphyroblasts with inclusions of quartz, biotite, plagioclase, K-feldspar, hercynite, or a combination of these phases. In the leucocratic lenses, the garnets range from anhedral to euhedral, commonly with only quartz, hercynite, and biotite as inclusions. In both occurrences, the garnets may predominate and make up 70% of the rock over a small area (e.g. a layer less than 3 cm thick)

Hercynite occurs as dark green to brown anhedral to euhedral crystals observed only under the microscope (figures 4.8, 4.9). It is generally isolated from quartz by cordierite - K-feldspar mosaics, and to a lesser extent by biotite, sillimanite, or garnet.

Corundum is rare and occurs as tiny anhedral to subhedral grains. It is invariably corroded and/or altered. Cordierite, hercynite, biotite, muscovite, and K-feldspar are commonly associated.

Orthopyroxene is present as anhedral to euhedral grains rarely up to 3 cm across. Rarely, grains seem to have undergone two distinct episodes of growth, as they have

Fig. 4.7. Hand samples showing leucocratic segregations containing abundant garnet and melanocratic zones rich in biotite and lacking garnet. Upper right sample is cut surface. Penny for scale. Sample locality 20.

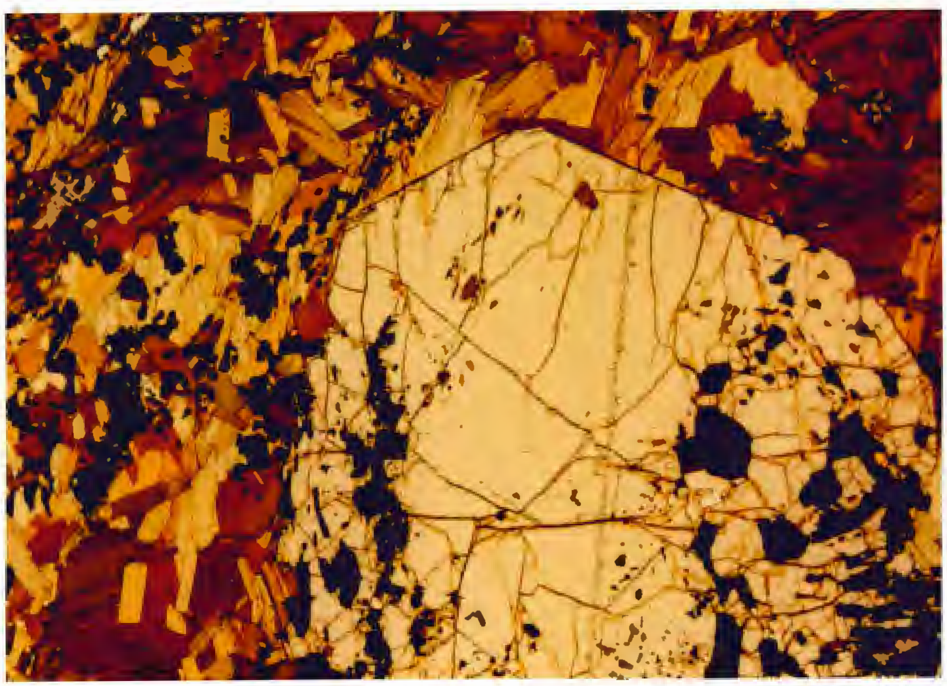

Fig. 4.8. Photomicrograph of garnet porphyroblast surrounded by biotite. Green spinel (dark green to black) occurs as anhedral grains. Sample 6-1. Plane light. Photo is 9 mm across.

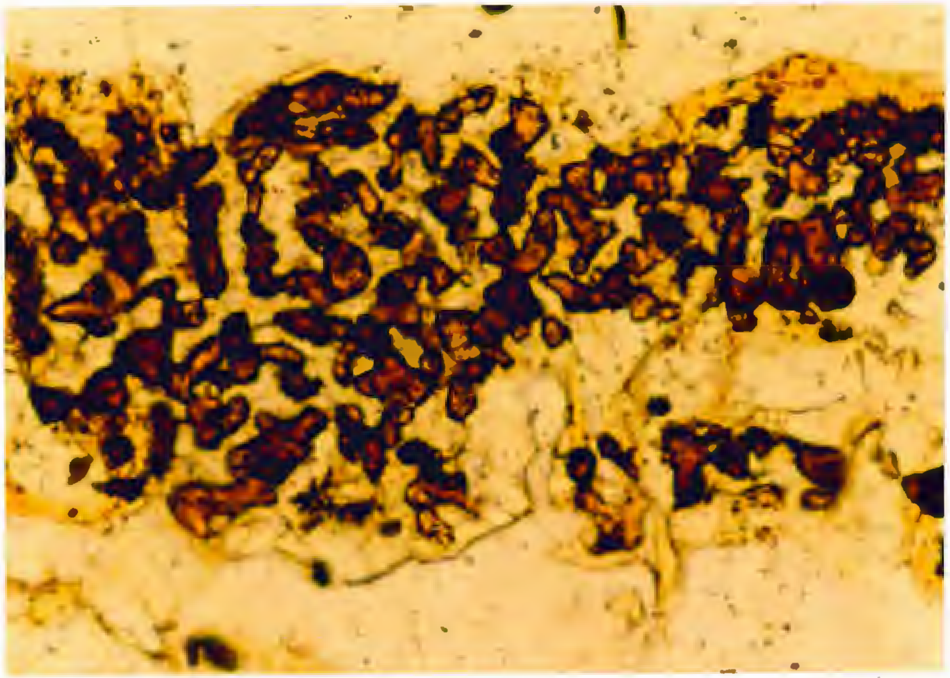

Fig. 4.9. Photomicrograph of brown spinel encased in a sheath of cordierite which, in turn, is surrounded by K-feldspar and quartz-rich matrix. Sample 35-9. Plane light. Photo is 0.5 mm across.

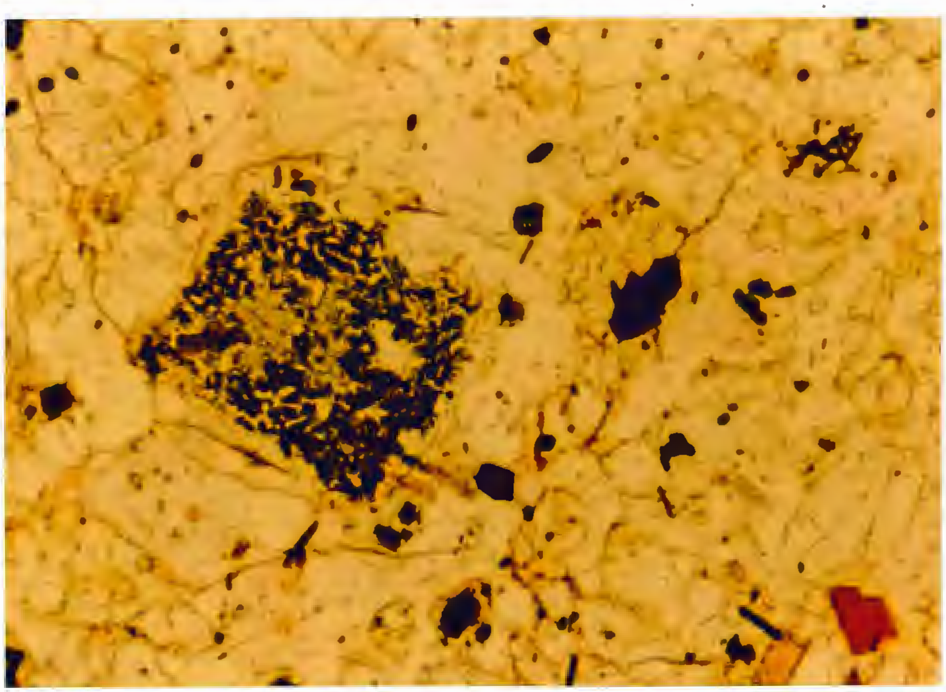

Fig, 4.10. Photomicrograph of a pseudomorph now composed of green spinel, sillimanite (high relief), and cordierite in a matrix of K-feldspar, quartz, and biotite. Sample 35-9. Plane light. Photo is 3.5 mm across.

optically continuous overgrowths (figure 7.5). Orthopyroxene is associated with K-feldspar, quartz, biotite, cordierite, and hercynite.

Zircon, rutile, graphite, and opaque oxides (magnetite and/or ilmenite) occur in most samples. Tourmaline and staurolite (a single corroded grain was found) are rare. Textural relations indicate muscovite and chlorite are late.

The rocks of this unit are typically foliated. They also exhibit a tendency for large porphyroblasts (e.g. garnet, K-feldspar, or orthopyroxene) and/or cordierite - spinel ± sillimanite intergrowths pseudomorphing earlier porphyroblasts (figure 4.10).

INTRUSIVE IGNEOUS ROCKS

SQUAW MOUNTAIN GRANITE

The Squaw Mountain granite is a white to pink, medium- to coarse-grained, heterogeneous, poorly to well-foliated porphyritic biotite granite. Biotite flakes define the foliation. Locally, randomly oriented megacrysts of microcline commonly 5 cm across stand out in relief on weathered outcrop. Zones of sheared Squaw Mountain granite show progressive reduction in the grain size of feldspar and quartz, forming augen gneiss, grading into mylonitic rocks (now blastomylonites) which contain ribbons of quartz several cm long parallel to foliation (e.g. figure 3.2). The granite body is cut by easily weathered amphibolite dikes which are marked by linear depressions in outcrop. The granite contains K-feldspar, quartz, plagioclase, biotite, and minor zircon, apatite and opaque oxides.

RED MOUNTAIN SYENITE

This unit grades from a hornblende syenite to a hornblende granite with minor biotite. The syenite occurs mostly south of the study area whereas the granitic phases occur dominantly as sills which interfinger with the Bluegrass Creek suite.

The Red Mountain syenite is a rusty brown weathering, greenish grey, medium to coarse-grained hornblende-olivine-clinopyroxene bearing syenite. The most distinguishing characteristic of this unit is the common occurrence of olivine and clinopyroxene rimmed by hornblende (figure 4-11). All outcrops are deeply weathered, resulting in bright red cores (weathered olivine and clinopyroxene) in most hornblende crystals. The mineralogy of this unit is microcline (slightly perthitic), hornblende, olivine, clinopyroxene, quartz, and characteristic abundant zircon, $\pm$ biotite, $\pm$ magnetite, $\pm$ ilmenite, $\pm$ allanite.

The syenite grades into granite with increasing modal quartz. Some granite sills adjacent to pelitic units contain abundant biotite, less hornblende, and no olivine or clinopyroxene near the contact with the country rock.All phases of the RMS contain high concentrations of zircon. The

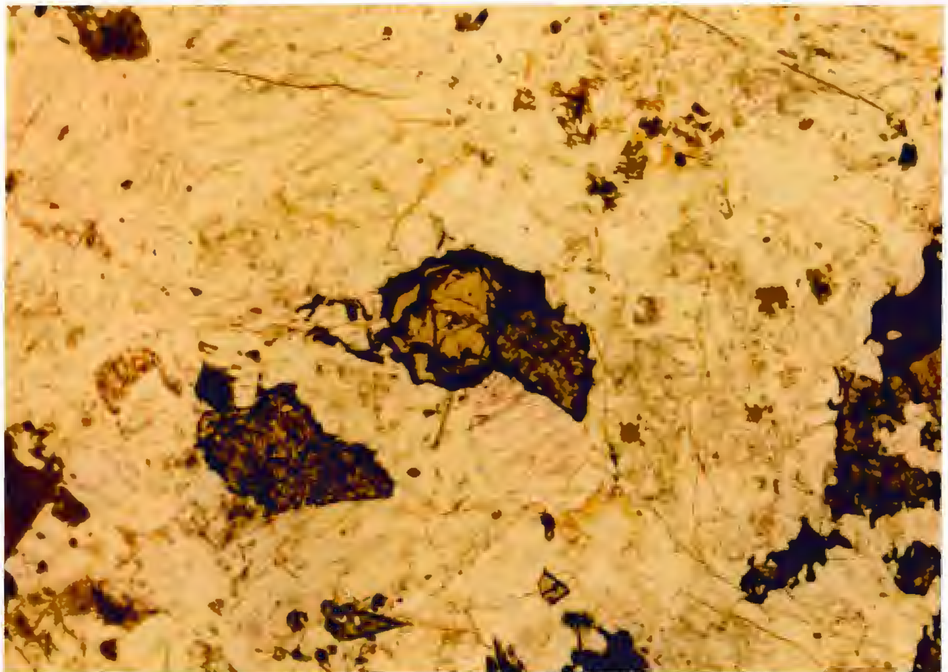

Fig. 4.11. Photomicrograph of Red Mountain syenite. Olivine and clinopyroxene (high-relief) are rimmed by hornblende (dark). The matrix consists of K-feldspar and biotite. Sample 44-1. Plane light. Photo is 9 mm across.

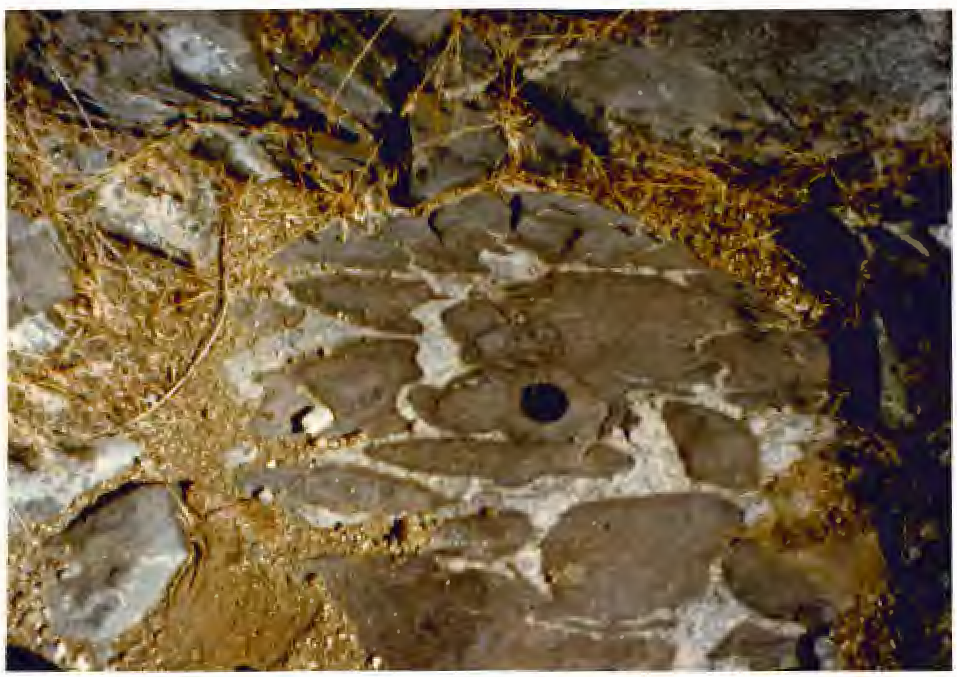

Fig. 4.12. Mixed dikes. Small pods of amphibolite in a granitic matrix. Lens cap for scale.

granites grade laterally into pegmatites composed primarily of K-feldspar, quartz, and biotite. Much of the K-spar here is light green to blue amazonite, and much of the pegmatite consists of graphic intergrowths of amazonite and/or albitic plagioclase with quartz.

COMPOSITE DIKES

This unit consists of amphibolitic dikes and composite dikes where mafic liquids and granitic liquids comingled with variable amounts of homogenization. The rocks vary from almost entirely mafic to roughly equal amounts of mafic and felsic material (figure 4.12). The mafic zones are largely plagioclase, hornblende, biotite, and clinopyroxene whereas the felsic zones contain quartz, plagioclase, orthoclase, biotite, and zircon. These dikes cross-cut the RMS and may result from mixing of late mafic phases of the LAC and late granitic liquids of the RMS.

CHAPTER 5: METAMORPHISM OF PELITES

General Statement

The pelitic rocks of the Bluegrass Creek Suite contain mineral assemblages which are largely a product of the contact metamorphism associated with the intrusion of the Laramie Anorthosite Complex. In order to gain a better understanding of the contact effects, it is necessary to first consider the textural and mineralogic state of the rocks prior to this event. These rocks, having undergone amphibolite facies metamorphism at about 2.6 b.y., might be expected to retain some of the textures and some of the compositional heterogeneities produced during that metamorphism (e.g. large porphyroblasts). A brief overview of the regionally metamorphosed rocks from west of the study area is presented first, to provide a basis from which the textural and mineralogical effects the intrusion of the Laramie Anorthosite Complex might be separated from those features which originated during earlier regional metamorphism.

Regional Terrain

The pelitic rocks in the regionally metamorphosed terrain are characterized by the amphibolite grade assemblage: Qtz-Pfs-Mus-Als-Bio-Gar-Sta (see Appendix 1 for explanation) (Grant & Frost, 1986, Hodge, 1966). The aluminosilicate minerals present are kyanite and fibrous sillimanite. Kyanite crystals are locally quite large, reaching lengths of 5 cm. Fibrous sillimanite defines a late foliation and may be the result of a reaction involving the breakdown of quartz + muscovite ± staurolite (figure 2.1). A process for the production of a fibrolite foliation has been proposed by Vernon (1987) who suggests that fibrous sillimanite may form through cation leaching of muscovite in zones of high non-coaxial strain. Fibrolite would be concentrated in these zones because of its ability to withstand non-coaxial deformation through grain-boundary sliding (fibre sliding) without the formation of significant amounts of dislocations. This process may operate independently or as part of the previously described reaction involving the breakdown of quartz-muscovite (figure 2.1).

The coexisting kyanite and sillimanite suggest that the metamorphic path in P-T space crossed the polymorphic transition between kyanite and sillimanite. Rarely, kyanite is partially replaced by sillimanite, and thus it is inferred that the kyanite probably formed relatively early and fibrolite most likely formed later, during the thermal culmination of the amphibolite grade event (Grant & Frost, 1986; Hodge, 1966). (Andalusite is restricted to within 2 km of the RMS).

Staurolite, abundant in the regional terrain, forms large subhedral to euhedral porphyroblasts up to 5 cm. or more in length (Bothner, 1966, Hodge, 1965). These large crystals commonly contain abundant inclusions of quartz.

Garnets also occur as large subhedral to euhedral porphyroblasts, commonly with diameters of 3 cm or more. Geobarometry on coexisting garnet (cores) - plagioclase - aluminosilicate - quartz (Newton & Hazelton 1981) by Grant and Frost (1986) suggests pressures of 6.0 $\pm$ 0.5 kb., whereas garnet - biotite geothermometry (Ferry & Spear, 1978) on rocks from the same area yield temperatures of approximately 600 degrees C. Further microprobe study of clear Fe-rich rims on these garnets yield evidence for subsequent decompression to about 3 kb. (Grant and Frost, 1986). Andalusite replacing kyanite in associated rocks supports this interpretation.

Metamorphic Isograds, Grade, and Zones

Metamorphic isograds are by definition, lines (in 2-D) or surfaces (in 3-D) of equal metamorphic "grade". Although the term "metamorphic grade" is not rigorously defined, it can here be directly related to pressure, temperature and to the composition of the coexisting fluid. In this study, the nature of the metamorphism suggests that variations in pressure had the least effect on relative "grade". In modeling the system, an isobaric

T-X diagram is used to account for observed changes in metamorphic grade.

The isograds mark the boundaries between metamorphic zones. Metamorphic zones are defined as zones which contain a characteristic mineral assemblage or assemblages. An isograd on the low grade side of a metamorphic zone marks the appearance of a new mineral or mineral assemblage, and the isograd on the high grade side will mark the beginning of a new zone with a new mineral or mineral assemblage which is unstable in the previous metamorphic zone.

Ideal Phase-Equilibrium Models

The first appearance of a new mineral assemblage (assuming constant bulk compositions) is taken as evidence of reaction between previously stable (or metastable) assemblage(s). When an assemblage becomes unstable and reacts due to changes in intensive variables (i.e. pressure, temperature, fluid composition), the new assemblage will ideally contain the new minerals produced and the non-limiting reactants. Consider the hypothetical phases A,B,C, and D in the reaction, A + B = C + D, with limiting amounts of A, reacting to the right. The new assemblage is B + C + D. A and B together are unstable in the presence of both C and D, except under equilibrium conditions for the reaction.

"Real" Phase Equilibria and Potential Pitfalls

In natural systems, things are not so simple. For example, compositional variation in a single phase can drastically broaden the temperature interval over which a given reaction appears to take place. The first appearance of the new assemblage (e.g. C + D) does not necessarily involve the disappearance of the old assemblage (e.g. A + B). Evans and Guidotti (1976) present a classic study in which assemblages, which in the simplest case are univariant, persist for several km past the isograd marking the new metamorphic zone. In real systems, the beginning of a new assemblage need not mark the disappearance of another, only the beginning of the end.

The interpretation depends on real rocks and real systems. The choice of an adequate system in which to model a group of real and chemically complex rocks requires many judicious assumptions. The limitations inherent in this choice should be kept in mind through all interpretations. In most cases when the model system fails to predict observations, the system may not be fully understood, or the need to simplify the natural system in order to model it is evidence for the consideration of an insufficient number of variables. In the latter case, observations, experiments, and calculations aid in determining the effects of additional components in a model system.

The Phase Rule

The phase rule, $f = c + 2 - p$, states that the degrees of freedom equals the number of components plus 2, minus the number of phases. Therefore, one way for an assemblage to exist well past the model system isograd is for the real system to contain an additional component (e.g. Ti in biotite) and therefore an additional degree of freedom. The addition of a phase with two new components (plagioclase could introduce 2 components, Ca and Na, while only adding one phase to the system) would produce a degree of freedom. This extra degree of freedom can permit assemblages which would represent univariant reactions to occur over a significant range of P-T-X conditions (a volume in P-T-X space).

Geometry of Isograds

Ideally, in thermal metamorphism, the metamorphic isograds and the metamorphic zones are concentric about the heat source, and though the isograds can mimic irregularities in the contact, small irregularities are commonly subdued by conductive transfer of heat through rock. Locally, irregularities in isograds are produced by zones of high fluid flow (advection) which carry heat into the country rock (e.g. via veins and faults).

Metamorphic Facies

A metamorphic facies is defined by a set of mineral assemblages such that there is a predictable relation between bulk composition mineralogy. The mineral assemblages are generally taken to reflect the conditions of metamorphism.

The standard facies classification loses its applicability in small-scale studies, where significant changes in the rocks might not be represented by changes of facies. In small-scale studies, the same principles are employed, and the investigator can determine how much to divide or combine the rocks under consideration by considering only a limited range of bulk compositions at a time. The rocks in the present study area may fall into one or more of three standard facies: 1) upper amphibolite; 2) lower granulite; and 3) pyroxene hornfels. However, subfacies displayed primarily in figure 5.1 will reflect the subtle changes in a more useful way.

Bluegrass Creek Suite

Discussion of the progressive contact metamorphism of the pelitic rocks within the Bluegrass Creek Suite is presented beginning with rocks displaying the lowest-grade assemblages in the study area, those furthest from the contact. These rocks contain very little staurolite (a single corroded grain was found) and are interpreted to

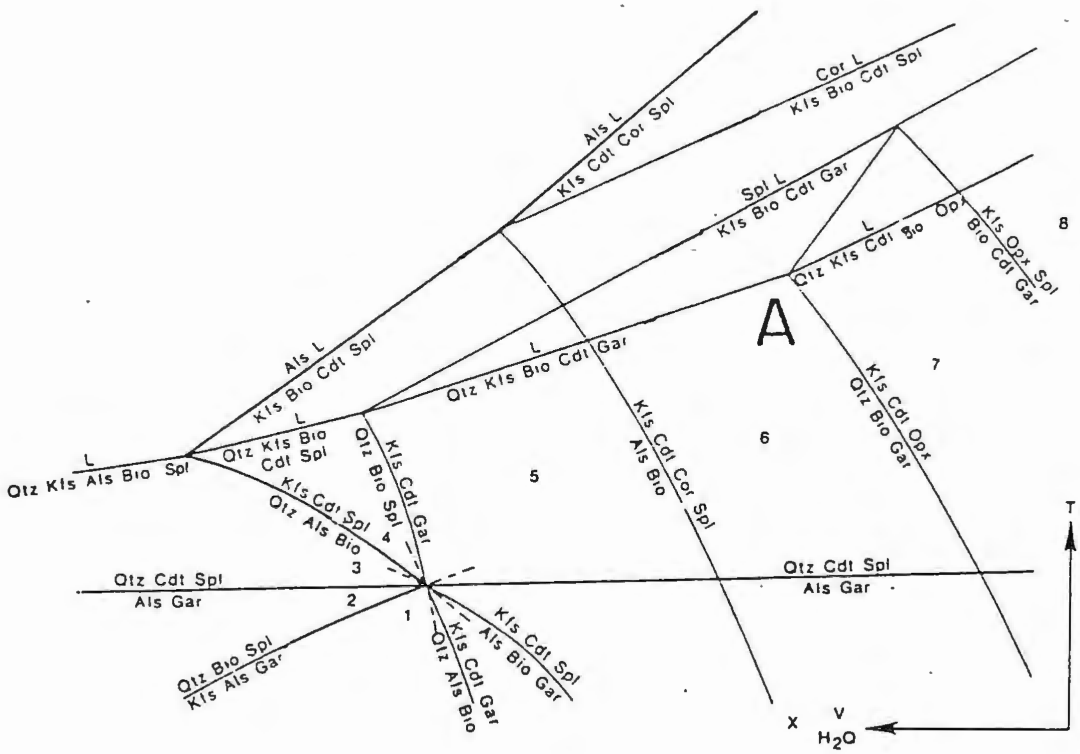

Fig. 5.1. Schematic isobaric T-X(H_2O) diagram of some equilibria pertinent to the development of the assemblages in the Bluegrass Creek Suite (modified after Grant, 1985, fig. 13).

reflect conditions above the breakdown of staurolite by the reaction:

Qtz + Mus + Sta = Bio + Als + Gar + Vap (figure 2.1)

The presence of zinc in staurolite can increase its stability field significantly (Guidotti, 1970), thus a single grain of staurolite (all that was found in this study) need not affect interpretation of grade.

Many samples contain appreciable muscovite, perhaps left over from the breakdown of staurolite. However textural evidence indicates most, if not all Qtz-Mus assemblages are retrograde. Finally, the widespread occurrence of K-feldspar with sillimanite indicates conditions above the reaction:

Qtz + Mus = Kfs + Als + vapor (figure 2.1).

Muscovite, however, is locally in contact with quartz and due to the uncertainties in interpretation of metamorphic textures, cannot be ruled out as a prograde phase. Some of the muscovite may be pre-contact metamorphism which failed to react with quartz (ie. quartz may have been absent locally). The presence of muscovite may indicate significant local variation in X_{H2O} and/or compositional variation in any of the phases (e.g. Na substitution for K in muscovite or K-feldspar); Both are consistent with the observed association of all four phases some distance past the first appearance of K-feldspar- sillimanite.

Where muscovite is associated with corundum, it is clearly retrograde, and probably formed through the reaction:

K-feldspar + Corundum + Vapor = Muscovite (Figure 2.1).

As the Laramie Anorthosite Complex contact is approached, five distinct isograds can be mapped. Grant (1985a) constructed a petrogenetic grid for the system KFMASH to aid interpretation of the assemblages found in the Morton Pass area (figure 5.1). Morton Pass lies along the western contact of the Laramie Anorthosite Complex approximately 45 km southwest of the Bluegrass Creek area (Figure 1.2). This schematic isobaric petrogenetic grid in T - X_{H2O} space is useful (with minor modification) to the rocks of the Bluegrass Creek Suite. T-X_{H2O} space is used for three reasons; (1) due to the abundance of carbonates, any coexisting fluid should not be modelled as pure H_2O, (2) assumed low variations in pressure during the metamorphism probably had minimal effect on the reactions, and (3) the effects of temperature and coexisting fluid composition (relative to pressure) become especially important in the production of melts.

Determination of Metamorphic Grade

The placement of metamorphic isograds was determined using the first appearance of a new equilibrium assemblage. In determining equilibrium, grain-to-grain-contact was considered prime evidence. In cases where three phases were to be considered at equilibrium, a search was made for a triple point where all three were in contact. Finally, where the new equilibrium assemblage was defined by four coexisting minerals, the coexistence of the four possible three-phase assemblages was considered sufficient to define the equilibrium.

CONTACT-METAMORPHIC ZONES

A list of the major minerals present in each zone, as well as the "key" equilibria used in determining the appropriate facies, is contained in the text. For a sample-by-sample listing of mineral species present and interpreted equilibrium assemblages, see appendix A-1.

Kfs-Als-Gar Zone

The rocks most distant from the contact representing the lowest grade of contact metamorphism contain the minerals:

Qtz-Kfs-Pfs-Als-Bio-Gar-Spl

and the important assemblages are:

Kfs-Als-Gar, Qtz-Als-Bio, and Qtz-Bio-Spl

The assemblages are conspicuous in their lack of cordierite.

The rocks are typically well foliated and retain textures indicative of the regional metamorphism. For example, large porphyroblasts of garnet are enclosed in sillimanite folia. Sillimanite (prisms, needles, and fibrolite) is deflected around the porphyroblasts (figure 5.2). Sillimanite prisms and needles are strain free, indicating growth after the deformation and/or subsequent static recrystallization.

Possible sillimanite producing reactions include (1) the breakdown of quartz- muscovite, (2) the recrystallization of fibrolite or other aluminosilicate minerals, or (3) a combination of both processes. The morphology of the sillimanite suggests that it formed from an earlier foliation and that it replaced a very platy or elongate Al-rich mineral (e.g. muscovite).

In "strain shadows" of some garnets K-feldspar is abundant (figure 5.2). Equilibrium of the Kfs-Als-Gar assemblage is certain. Further petrographic study of the same thin section reveals the assemblage Qtz-Bio-Spl (most commonly as polyphase inclusions in the garnet porphyroblasts) whereas rocks from the same outcrop yield the equilibrium assemblage Qtz-Als-Bio. Relating these equilibrium assemblages to figure 5.1, it is apparent that the rock equilibrated near the isobarically univariant curve representing the reaction:

Kfs + Als + Gar = Qtz + Bio + Spl

and temperatures below the reaction

Als + Gar = Qtz + Cdt + Spl

In the present study, this assemblage is found only in the NW corner of the study area (plate 2).

Kfs-Cdt-Spl Zone

The first definable isograd marks the first appearance of rocks which in the field were mapped as "blue-buff" gneisses. These rocks were dark grey to black with a blue cast due

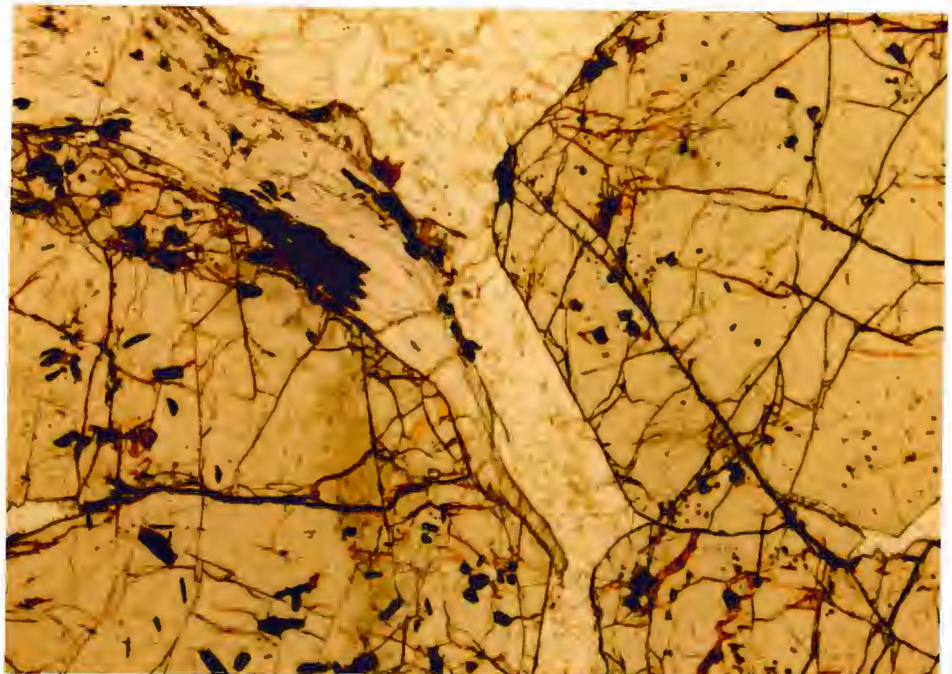

Fig. 5.2. Photomicrograph of K-feldspar (low-relief), sillimanite (moderate-relief) and garnet (high-relief) assemblage. Inclusions are biotite and spinel. Sample 9-2. Plane light. Photo is 9 mm across.

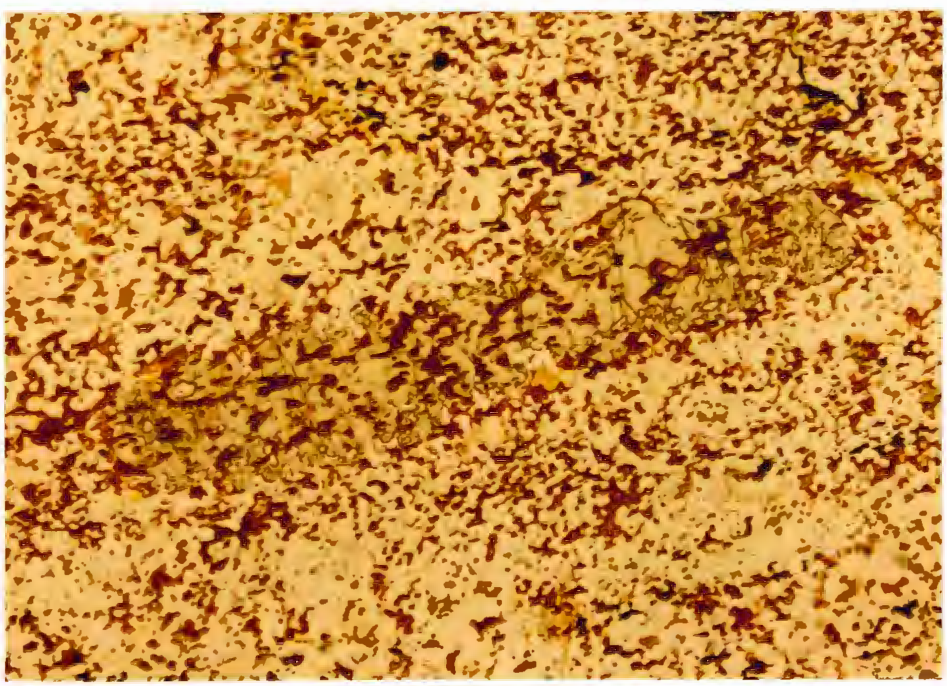

Fig. 5.3. Photomicrograph of "prismatic" garnet. Matrix is quartz, K-feldspar, and biotite. Sample 34-7. Plane light. Photo is 9 mm across.

primarily to abundant cordierite. The buff color results from weathering of veinlets, pods and lenses of K-feldspar-rich material. The major minerals present include:

Qtz-Kfs-Pfs-Als-Bio-Cdt-Gar-Spl

The zone is distinct in that garnet and aluminosilicate, often abundant in the same rock, are not found in contact. This suggests temperatures above the vapor-absent reaction Als + Gar = Qtz + Cdt + Spl.

The isograd is more succinctly defined by the first appearance of Kfs-Cdt-Spl (zone 4, figure 5.1). These phases were typically found in pods or elongate blebs where intergrowths of Cdt-Spl $\pm$ Als, $\pm$ Bio, are enveloped by K-feldspar. Occasionally in thin section these intergrowths defined geometric (crystal) outlines (e.g. squares, parallelograms, and rectangles) indicating pseudomorphous growth after some earlier mineral(s) (e.g. figures 4.4, 4.10).

These pseudomorphs can be explained in a number of ways, the simplest being is pseudomorphous growth after an aluminosilicate phase. In the regional terrain it is not uncommon for large kyanite and sillimanite to contain abundant inclusions of biotite and quartz. In the presence of quartz and biotite, the inferred reaction from figure 5.2 would be:

Qtz + Als + Bio = Kfs + Cdt + Spl

One cannot rule out the possibility of staurolite or even sapphirine as possible precursors. The preserved crystal form is in some cases compatible with those exhibited by either staurolite or sapphirine. In considering either of these possibilities, the major obstacle is there are no relics left within the pseudomorphs to indicate their earlier presence. Without these relics. Arguments based on shape and the bulk composition of pseudomorphs is rarely conclusive, especially since in determining an appropriate bulk composition, the possibilities of inclusions (staurolite in the regional terrain is commonly full of quartz inclusions), the distance across which diffusional processes were effective, and whether the mineral could be stable at conditions attained in the rocks must be considered.

Staurolite is a possibility; It is abundant in the regional terrain and its crystal form is similar to some observed pseudomorphs. The stability field for sapphirine-orthopyroxene assemblages is appropriate for metamorphic conditions near the contact. However, the lack of relics and the high Fe-content of the pseudomorphs demand it be considered a remote possibility.

One might argue for two distinct sources for the pseudomorphs by citing the two distinct spinel types (figures 4.4, 4.9, and 4.10). Both brown and green spinel occur in pseudomorphs and probably have high Fe content (both ferric and ferrous). The green spinels are rich in hercynite component (Grant, pers. comm., 1986) whereas compositions of brown spinels are not well constrained but are likely to be richer in Fe^{3+}. This suggests that the cordierite-spinel intergrowths, with different colored spinels (having different amounts of ferric and ferrous iron) may represent two distinct precursors.

These observations indicate that most pseudomorphs probably represent the breakdown of an inclusion rich aluminosilicate mineral. However, staurolite is a likely candidate for some, whereas original sapphirine is unlikely.

If the petrogenetic grid (figure 5.1) is applied to these rocks, they plot on or above the reaction in which:

Qtz + Als + Bio = Kfs + Cdt + Spl

The assemblage Qtz-Als-Bio extends past the isograd marking the first appearance of Kfs-Cdt-Spl which probably corresponds the invariant point (#1) in figure 5.1. Also, Qtz-Als-Bio appear to be in equilibrium well past the next isograd, probably due to variations in the composition of the real system (e.g. Ti in biotite) versus that of the simplified model system.

Kfs-Cdt-Gar Zone

The next mapped isograd is defined by the first appearance of the equilibrium assemblage Kfs-Cdt-Gar. In outcrop these rocks again have the characteristic blue-buff color. However, the percentage of leucosome (light colored material consisting dominantly of feldspar and quartz, with or without biotite and/or garnet) in outcrops south of the isograd is higher than in the outcrops north of the Kfs-Cdt-Gar isograd. Commonly garnet is incorporated into the leucosome or isolated from the rest of the rock by the leucosome. The major minerals present in this zone are:

Qtz-Kfs-Pfs-Als-Bio-Cdt-Gar-Spl

The key equilibria are:

Kfs-Cdt-Gar, Kfs-Cdt-Spl, Als-Bio,

whereas the assemblage Als-Gar is absent, placing these rocks on or above the reaction:

Qtz + Bio + Spl = Kfs + Cdt + Gar

in zone 5 of figure 5.1.

The textures in these rocks are quite variable. Garnet growth is restricted to distinct layers, probably due to local compositional differences, and rarely appears to have a prismatic habit (figure 5.3). Spry (1969) notes that garnet pseudomorphs after orthopyroxene are common in syenitic charnockites. More commonly garnet occurs as subhedral to euhedral grains up to 2 centimeters across with polyphase inclusions (e.g. Qtz-Bio, Bio-Spl). Finally, it is found as corroded grains in layers with abundant quartz and magnetite (a possible restite?).

Cordierite generally makes up 5 - 15% of the rock and occurs as subhedral to anhedral grains. K-feldspar, quartz, aluminosilicate minerals, and biotite in varying amounts comprise the bulk of the matrix. Pods and lenses of Spl-Cdt ± Als are common, although the spinel and aluminosilicate appear to be more entrenched in the larger cordierite mosaics and increasingly isolated from quartz than in lower grade rocks.

Kfs-Cdt-Cor-Spl or Corundum Zone

The first appearance of corundum defines the fourth mappable isograd. Finding all four phases Kfs-Cdt-Cor-Spl in grain-to-grain contact was impossible. The designation of this zone is a bit tenuous and should perhaps be labeled the corundum zone. The most convincing evidence of the equilibrium of the four-phase assemblage is shown in figure 5.4. Here the four phases (Kfs, Cdt, Cor, Spl) are present with sillimanite. In figure 5.1, the reaction involved in the production of the corundum-bearing assemblages is:

Als + Bio = Kfs + Cdt + Cor + Spl

A more common assemblage suggests an alternative reaction in the production of corundum. Corundum is typically associated with silica-poor, K-feldspar-rich areas in thin section. Retrograde muscovite also occurs in such zones. The reaction involving the breakdown of muscovite in the absence of quartz (figure 2.1):

Mus = Kfs + Cor + vapor

may have produced the bulk of the corundum in the area.

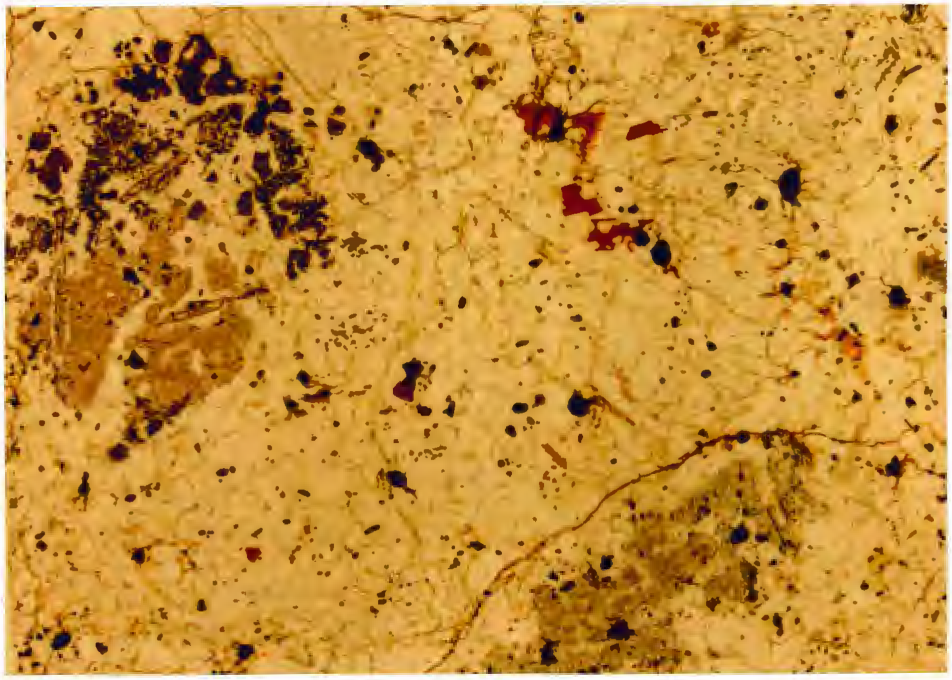

Fig. 5.4. Photomicrograph of pseudomorph with the critical assemblage: K-feldspar-cordierite (low relief)-spinel (dark granular)-corundum (high relief bladed)-sillimanite (high relief blocky). Sample 35-9. Plane light. Photo is 9 mm across.

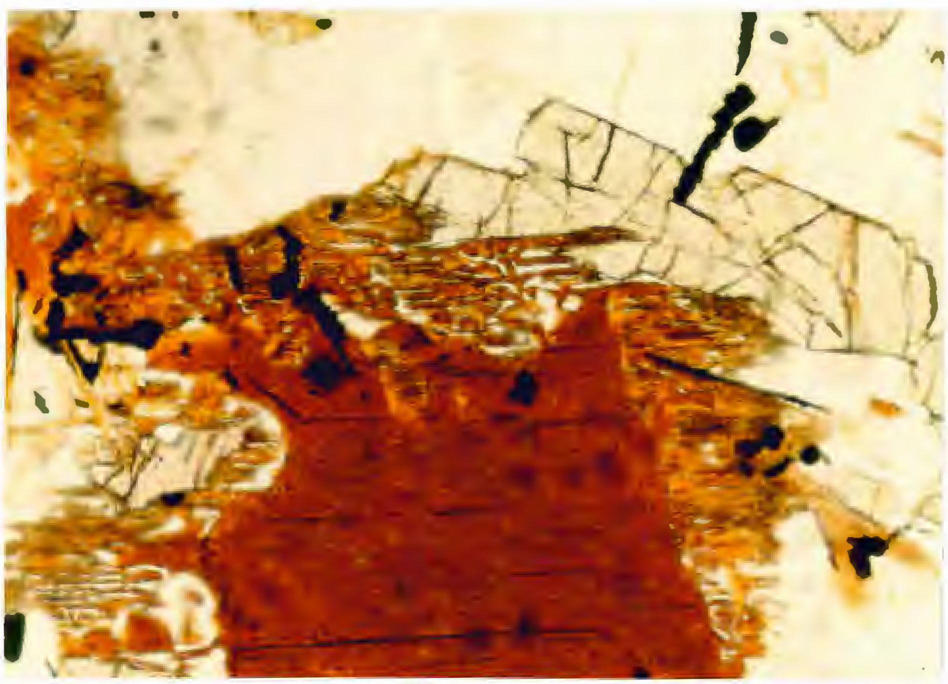

Fig. 5.5. Photomicrograph of "vermicular" biotite (brown) intergrowth with K-feldspar (low relief) and orthopyroxene (high relief). Sample SB-8. Plane light. Photo is 1.5 mm across.

The major minerals present in this zone are:

Qtz-Kfs-Pfs-Mus-Als-Bio-Cdt-Cor-Gar-Spl

These rocks are texturally very similar to the rocks of the previous two zones. Many of the cordierite-spinel knots are present. Aluminosilicate and biotite still coexist, but without quartz, and this association becomes less common towards the contact with the Laramie Anorthosite Complex.

Leucocratic lenses (leucosomes) are quite common in this zone and are locally make up a majority of the rock. These lenses and layers are typically the only places in the rock in containing garnet.

Kfs-Cdt-Opx Zone

The presence of orthopyroxene in equilibrium with cordierite and K-feldspar marks the beginning of the next metamorphic zone. The corresponding isograd is based on only a few outcrops and is not well constrained except in the central part of the field area. Outcrops are darker and contain significantly less garnet and leucocratic material than in the previously discussed zones. The major minerals present in this zone are:

Qtz-Kfs-Pfs-Als-Bio-Cdt-Gar-Opx-Spl

The disappearance of some phases is noted. First, muscovite is not found in any of the samples from this zone. This may be due to insufficient outcrop or sampling, or it might indicate that the rocks in this isograd have not suffered the same retrograde reactions that had affected the previously-mentioned muscovite-bearing assemblages. A third and preferred reason for the absence of muscovite is that the bulk compositions were too Fe-rich. Thus muscovite, and the mineral assemblages which might be retrograded to muscovite were never viable assemblages in these rocks. In such Fe-rich rocks, Al is tied up in garnet, cordierite, or spinel. The absence of corundum is consistent with this interpretation.

The first appearance of Kfs-Cdt-Opx may have occurred by the reaction:

Qtz + Bio + Gar = Kfs + Cdt + Opx + Vap

(figure 5.1). There are three reasons for this interpretation. First, the low abundance of garnet in the rocks of this zone is in direct contrast with the abundant garnet in the rocks of the earlier zones. Secondly, the garnets that are present are rather ragged, and appear to be relicts. Finally, the rocks characteristically contain the assemblage Qtz-Kfs-Bio-Cdt-Opx which is what would be expected if the limiting reactant were garnet.

Orthopyroxene and garnet are not found in equilibrium or in textural relationships that might indicate replacement. Instead, biotite grains rimmed by vermicular intergrowths with quartz and/or K-feldspar are associated with garnet and especially with orthopyroxene (figure 5.6). These intergrowths are not well understood and may have formed by orthopyroxene-producing reactions, as retrograde products of orthopyroxene, or by cotectic or peritectic crystallization from a melt.

The most striking textural change found in this zone is the presence of poikilitic grains of K-feldspar, and less commonly of quartz. The biotite within the oikocrysts is subhedral to euhedral in contrast its appearance as corroded grains elsewhere. The included grains of quartz, K-feldspar, and cordierite are commonly round and give the oikocrysts a "swiss cheese" texture. Elongate laths of plagioclase (figure 4.5) are rare.

Kfs-Opx-Spl zone

One isolated occurrence of Kfs-Opx-Spl was found in a large block (70 m across) of the Bluegrass Creek Suite within the Red Mountain Syenite, just south of Tunnel Road (plate 1). The major minerals present in the samples from this single locality (SB in plate 2) are:

Qtz-Kfs-Pfs-Bio-Cdt-Opx-Spl

These rocks also contain conspicuous amounts of graphite. The abundance of graphite implies a reducing environment and one in which H_2O is significantly diluted by other phases, especially CO_2 and/or CH_4 (Ohmoto and Kerrick, 1977; Frost, 1979).

Locally large knots (up to 3 cm across) of quartz and K-feldspar are present. Orthopyroxene grains are typically euhedral and locally reach lengths of 2 cm. Biotite occurs as large, unoriented grains, locally with abundant inclusions of K-feldspar, quartz, and orthopyroxene. Quartz and K-feldspar are also commonly poikilitic with inclusions of biotite, quartz, K-feldspar, and rarely cordierite or orthopyroxene.

This zone is characterized by textures which suggest crystallization from a melt. The details of these will be discussed in the chapter on partial melting.

Interpretation and Discussion

Interpretation of the textures and mineral equilibria is challenging because of the problems inherent in working with a silicate liquid phase. Drawing conclusions about a path through P-T-X space for a given rock is fraught with uncertainty, particularly when melting and subsequent segregation and/or crystallization may significantly modify the final texture. However, some points are worth noting.

First, the rocks north of the Kfs-Cdt-Spl isograd are likely to owe much of their present textural relations and at least some of their mineralogical assemblages to the earlier regional metamorphism. This seems evident from inclusion trails in garnet and textures suggesting pre- and syn-metamorphic growth (e.g. folia curving around porphyroblasts). However, recrystallization has modified many of the textures.

Secondly, it is evident that the development of a leucosome began near where the Kfs-Cdt-Gar zone was reached. Clearly the textures in the K-feldspar-cordierite gneisses suggest potential segregation and mobilization of a leucosome.

Continuing towards the contact with the RMS, the textures in the orthopyroxene-bearing rocks suggest crystallization from a rock which was partially molten. This is especially pronounced in the poikilitic textures found just north of and in the single locality south of the Tunnel Road.

Finally, partial melting in the rocks could serve to buffer the local temperature profile, and one would thus expect that the temperature would vary less drastically in areas where there is melt production. If this is happened, local variation in the composition of the fluid phase may have been a more significant factor than pressure or temperature.

It is theoretically possible to account for all but the lowest-grade assemblages found in the Bluegrass Creek Suite at constant temperature and pressure without invoking partial melting (e.g. an isothermal line through figure 5.1). However, a lack of a thermal gradient is highly unlikely, and as will be presented in the chapter on partial melting, an abundance of textural and mineralogical evidence suggests that indeed, partial melting did occur in rocks of appropriate compositions.

CHAPTER 6: METAMORPHISM OF OTHER ROCK TYPES

This chapter presents the information derived from marbles, calc-silicate rocks, and amphibolites. A list of minerals present in individual samples is presented in appendix B-1. Key equilibria are presented in the text. The metamorphism of the marbles and calc-silicate rocks are considered together; a discussion of the metamorphism of the amphibolites follows.

MARBLES AND CALC-SILICATE ROCKS

Due to the compositionally and spatially gradational nature of the marbles and the calc-silicate rocks, they are considered together. The metamorphic interpretations of these lithologies are limited to the determination of one isograd and two metamorphic zones. The major limiting factor is the lack of low variance assemblages. However, it may be related to the deficiency of reactions in the model system ($MgO-CaO-SiO_2-H_2O-CO_2$) over the range in pressure, temperature, and vapor composition for the formation of the Bluegrass Creek suite.

Regional Terrain

The marbles in the regional terrain are quite varied. Snyder (1985) describes several types including tremolite dolomite and a spotted dolomite-calcite marble in which the spots are serpentinized chondrodite. He reports that within 2.5 km of the contact with the Laramie Anorthosite Complex, the serpentine may be reconstituted into olivine.

Contact Aureole

The marbles and calc-silicate rocks in the study area are intimately associated with each other. The marbles are separated from other lithologies by zones of calc-silicate rock. Some of the marbles are well-foliated, this being especially evident in rocks with abundant phlogopite. Other marbles are essentially devoid of foliation (e.g. a well exposed marble quarry north of the Huston ranch). Even the calc-silicate rocks which contain abundant mica are for the most part coarse-grained and nonfoliated. This suggests recrystallization during the waning stages of the contact event when forces associated with the emplacement of the LAC had subsided and a static stress regime allowed recovery and a general coarsening of the minerals.

METAMORPHIC ZONES

The mineral equilibria for the two metamorphic zones distinguished during this study are shown schematically for the carbonate bearing assemblages in Figure 6.1. The main difference in the two diagrams is the breaking of the calcite-tremolite tie-line.

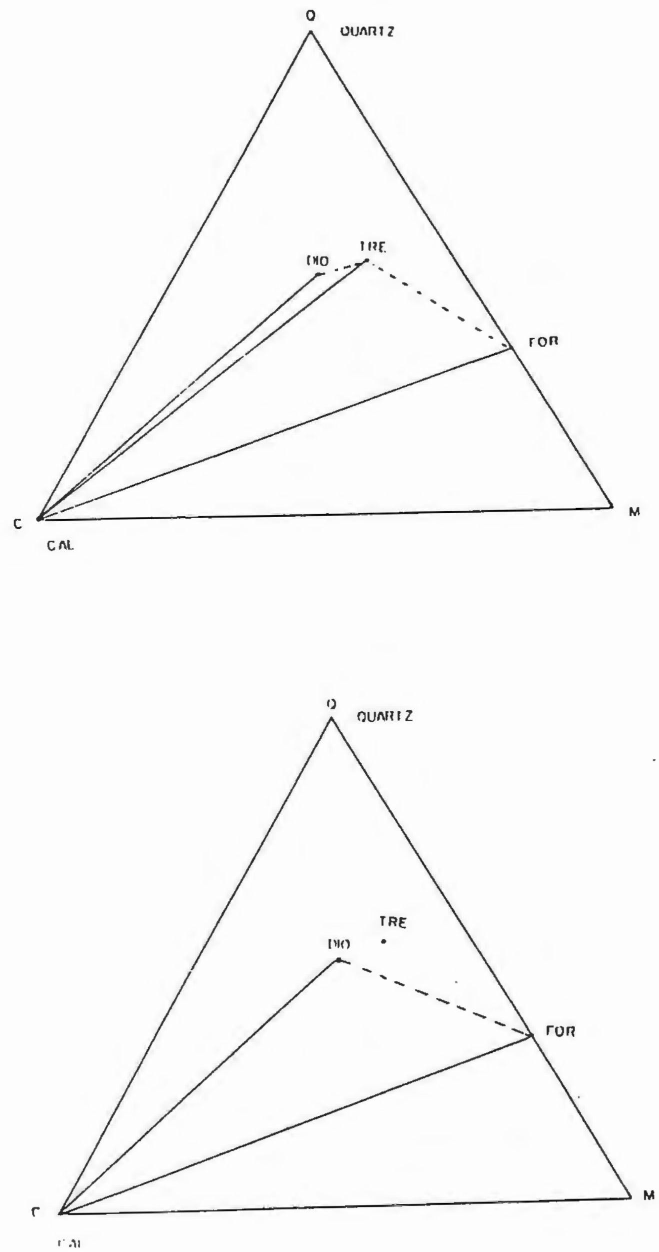

Fig. 6.1. QCM ternary plots (SiO_2-CaO-MgO) showing equilibrium phase relations for calcite bearing assemblages. Top diagram (lower temperature) shows tremolite-calcite stable. Bottom diagram shows breaking of the tremolite-calcite tie line (higher temperatures).

Tremolite-Carbonate Zone

The assemblage tremolite-calcite occurs only in marbles from the northern portion of the study area. These marbles may contain olivine (commonly retrograded to serpentine), diopside, phlogopite, and/or minor spinel.

These rocks are typically well foliated. The ease with which carbonates recrystallize, even at relatively moderate pressures and temperatures is well known. The foliation in the marbles is enhanced by the presence of silicate phases (especially phlogopite) and is sub-parallel to the contact of the Red Mountain syenite. It is inferred that the foliation is relict from the regional metamorphism, but has been rotated into parallelism by grain boundary sliding and recrystallization during the emplacement of the complex.

The most abundant marble type is a forsterite marble with the olivine partially to completely serpentinized, forming "ophicalcite". Schreyer (1976) suggests that the reactions producing this assemblage at 1 kb may be:

For $Xco_2 < 0.9$;

$$\text{1 Talc} + \text{5 Dolomite} =$$
$$\text{4 Forsterite} + \text{5 Calcite} + 1\ H_2O + 5\ CO_2$$

or for $0.9 < Xco_2 < .98$;

$$\text{Tremolite} + \text{11 Dolomite} =$$
$$\text{8 Forsterite} + \text{13 Calcite} + H_2O + 9\ CO_2$$

with a maximum at $X_{CO_2} = 0.9$. For $X_{CO_2} > 0.98$;

1 Diopside + 3 Dolomite =

2 Forsterite + 4 Calcite + 2 CO_2.

The second reaction is favored for the production of this assemblage for several reasons; 1) talc is rare, 2) Snyder (1984) reports marbles of the regional terrain are characterized by the assemblage tremolite-dolomite, 3) the second reaction requires a high X_{CO_2}. This is in agreement with the interpretation of the Red Mountain Syenite as a source of heat but not a source of significant amounts of H_2O. This allows the composition of the coexisting vapor to be effectively buffered locally by reactions occurring within the marbles.

The major minerals present in the carbonate bearing rocks in this zone are:

Cal-Tre-Dio-For-Phl-Srp-Spl, ±Dol±Czo

The key assemblages are Cal-Tre, Cal-For, and Cal-Dio.

In the model system $CaO-MgO-SiO_2-H_2O-CO_2$, these assemblages are mutually stable at temperatures in excess of 550°C (for $X_{CO_2} > 0.2$) at 3 kb (see Skippen, (1974, fig. 9). At 3 kb, the maximum temperature limit of the stability field for these assemblages is 650°C.

The calc-silicate rocks in this zone are characterized by the minerals:

Trem-Dio-Sph-Bio

with minor amounts of quartz or calcite (but not both).

Diopside-Forsterite Zone

The disappearance of tremolite from carbonate-bearing assemblages is the only mapped isograd (plate 2) in this study for carbonate and calc-silicate rocks. The rocks south of the isograd characteristically contain calcite with one or more of the silicate phases noted below. The minerals present include:

Cal-Dio-For-Phl-Srp-Spl-Sph-Czo

and the key mineral assemblages are Cal-For and Cal-Dio. Coexisting For-Dio has not been observed, but is suspected. Diopside and forsterite are relatively rare, however, Dio-Srp is found, and it is inferred that late serpentine-forming reactions have erased evidence for the assemblage.

The reaction producing the assemblage Cal-For-Dio may have involved the breakdown of tremolite-calcite to form the anhydrous silicate phases. One possible reaction is:

$$\text{Tremolite} + \text{Calcite} = \text{Diopside} + \text{Forsterite} + \text{Vapor}$$

$$3\ Ca_2Mg_5Si_7O_{22}(OH)_2 + 5\ CaCO_3 =$$

$$11\ CaMgSi_2O_6 + 2\ Mg_2SiO_4 + 3\ H_2O + 5\ CO_2$$

Skippen (1974) experimentally determined the location of this reaction at 3 kb in the presence of a mixed CO_2 - H_2O fluid. The isobaric curve in T-X_{CO_2} space has a maximum at $X_{CO_2} = 0.625$ and a temperature of just over 650°C. This fits in well with the current model where the pressures are inferred to be 3.0 ± 0.5 kb. This temperature agrees with those inferred from meta-pelites.

Retrogression

Most of the serpentine formed from olivine, though some may have formed by breakdown of other phases (e.g. diopside or chondrodite. Some serpentine has been redistributed in veins (Snyder, 1985). Elsewhere, olivine is partially or completely pseudomorphed by serpentine. This retrogression may be related to the release of water from crystallizing partial melts derived from the pelites.

Calc-Silicate Rocks

The calc-silicates of this zone are quite varied. The minerals found in this zone are:

Tre-Dio-Sph-Sca-Hbd-Bio-Czo-Cal-Chl-Gph.

and the common assemblages are Bio-Hbd-Dio and Sca-Dio-Sph-Gph. These rocks are commonly very coarse-grained, with euhedral crystals of biotite, clinopyroxene, and rarely long blades of scapolite.

AMPHIBOLITES

The amphibolites in the field area display little variation in mineralogy. The minerals present are:

Hbd-Pfs-Qtz-Bio- ± Gar ± Cpx ± Opx.

Interpretation of the metamorphism in these rocks suffers from lack of low-variance assemblages. However, some observations are significant.

Garnet appears only in the well-layered amphibolites found in the NW corner of the study area, where a substantial thickness of both massive and well-layered amphibolite is exposed (plate 1). Snyder's (1985) interpretation of the well-layered amphibolites as sub-aqueously deposited basaltic ash seems reasonable, for leaching of relatively mobile cations (e.g. Mg and Ca) from the ash during deposition, reworking, and burial could easily increase the relative alumina content, making possible the later formation of garnet. Massive amphibolites are interpreted as dikes or sills intruded into the volcanic pile (Snyder, 1985) and are conspicuous in their lack of garnet.

The garnets contain contorted inclusion trails of quartz with an ambiguous relationship with the crudely defined foliation. They appear to be pre- or syn- metamorphic and probably resulted from the regional event.

In rocks from the same area, "turkey-track" amphibolite (figure 4.1) is common in the well-layered amphibolites. This texture, with its long sprays of amphibole (some over 10 cm across) growing within distinct layers, may indicate growth in a homogeneous strain field, but the compositional layering clearly presents an important chemical constraint.

One sample has an altered diabasic texture. This unit, which occurs near the contact with the RMS, suggests that some amphibolites were indeed sills. The presence of rare orthopyroxene in these rocks may indicate a change in grade, but could also be a relict primary igneous feature.

CONCLUSIONS

Clearly, within the study area, the non-pelitic compositions are relatively insensitive to the thermal and compositional gradients developed during the thermal metamorphic event. A general coarsening and recrystallization is the principal textural evidence of the thermal event. The tremolite-out isograd in the marbles is the only mineralogical evidence for progressive metamorphism found in these compositions.

CHAPTER 7: PARTIAL MELTING

General Statement

The distinction between igneous and high grade metamorphic textures is typically quite subtle, especially in the case of high grade contact metamorphism where a pronounced foliation is commonly absent. In rocks which have partially melted and subsequently recrystallized, perhaps the most difficult questions to answer are; 1) which phases crystallized from the melt, 2) which phases, remained solid, and 3) what percentage of a given rock melted? Such interpretations are fraught with uncertainty since the rock is now 100% crystalline and cooling was too slow to produce finer-grained "chilled" textures in the melted fraction. Careful integration of macroscopic observations with the microscopic and experimental evidence is necessary to understand the process of partial melting.

A brief review of the macroscopic evidence for partial melting is followed by the microscopic observations. The importance of low-temperature melting compositions as they relate to the Bluegrass Creek suite are then discussed. Potential melt-producing reactions (consistent with experimental and theoretical considerations) are proposed to account for textures and mineralogies in the rocks.

Terminology

Johannes (1983) describes migmatites as "composite rocks consisting partly of gneiss or schist, and partly of portions having a plutonic appearance." Johannes also proposed a non-genetic terminology for migmatites. The gneissic or schistose part of the rock is known as the mesosome. The portion of the rock with a plutonic appearance is the leucosome because of its lighter color color (due to a higher proportion of felsic minerals than the rest of the rock). Commonly, the leucosome and the mesosome are separated by a relatively thin, dark zone richer in mafic minerals which is known as the melanosome.

Partial melting and mechanical segregation of the derived melt are processes which give rise to some migmatites. In zones from which significant partial melts have been removed, a relative increase in Fe, Mg, and Al and a relative depletion in Si and K is typically observed. The zones which are interpreted as the residua from which melt has been extracted are known as restites.

Macroscopic Evidence

The clearest evidence for partial melting is the obvious segregation of granitic liquids. Most migmatites described in the literature show centimeter- to meter-scale segregations, which are readily observed in outcrop and hand sample. These may be the result of significant partial melting and are characteristically observed in quartzofeldspathic migmatites.

The segregation displayed in quartzofeldspathic migmatites is often compelling, but the occurrences of this type of rock in the study area are rare. However, pelitic migmatites are common in the study area and worldwide, where they are probably more abundant than is reported in the literature. Most importantly, the bulk composition of meta-pelites varies widely. This reduces the likelihood of high percentages of partial melt at temperatures at or only slightly above the liquidus (ie. these are not likely to be eutectic compositions).

Disruption of foliation is generally considered an indicator for significant degrees of partial melting (McClellan, 1983). The meta-pelites of the BCS generally have a well defined layering in which lighter quartzo-feldspathic layers (commonly less than 0.5 cm thick) alternate with darker, cordierite- and/or orthopyroxene-rich layers which are generally more than 1.0 cm thick (figure 7.1). Areas in which the foliation is disrupted are considered to represent zones in which the percentage of melt reached a critical point and the foliation defined by the yet unmelted rock either failed brittly or became highly contorted as it responded ductily. Such zones commonly contain disoriented pieces of the mesosome or melanosome which still contain the earlier foliation.

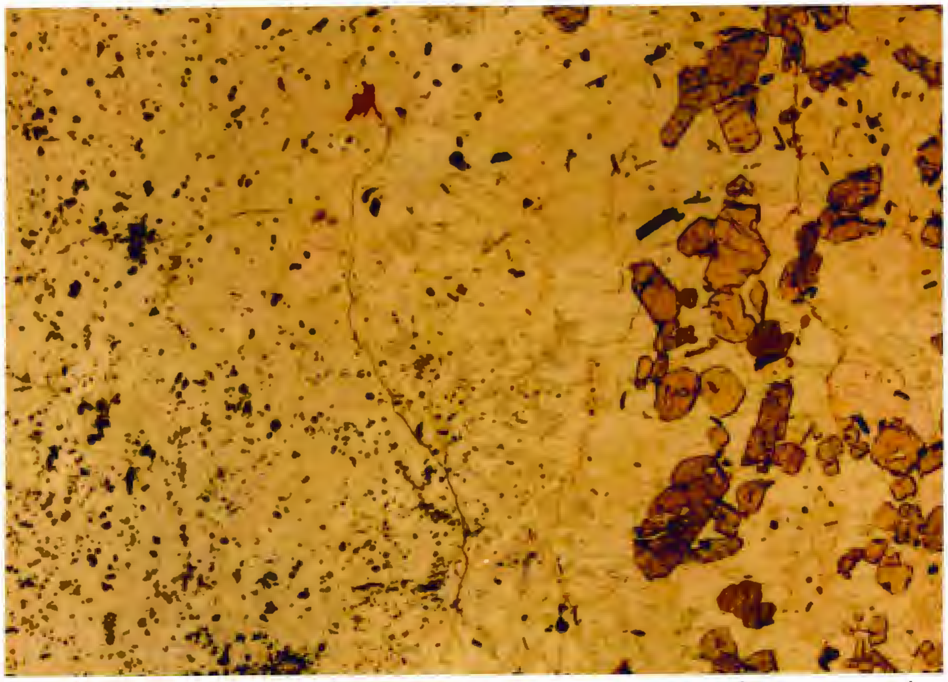

Figure 7.1. Photomicrograph showing distinct banding in metapelite. Left side is cordierite mosaic with less K-feldspar; Right side is an orthopyroxene-rich layer, with significant K-feldspar, quartz, and cordierite. Sample SB-3. Crossed polars. Photo is 9 mm across.

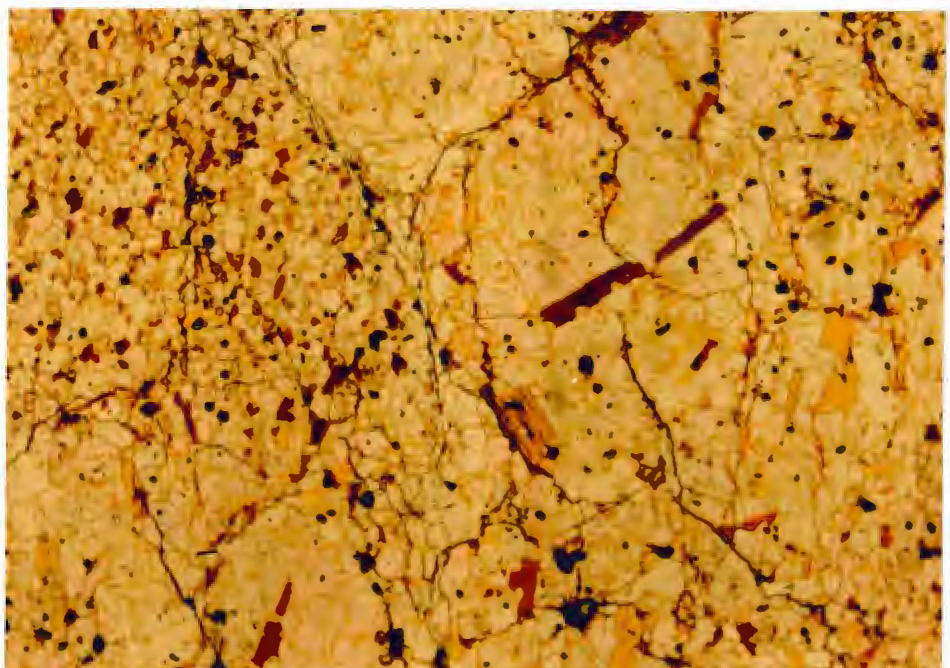

Fig. 7.2. Photomicrograph displaying bimodal biotite size and fabric. Note crude foliation present in small biotites whereas the large biotites are randomly oriented. Sample 35-2. Plane light. Photo is 9 mm across.

These zones are accompanied by stringers or small "dikes" (up to a few cm wide, but more commonly less than 0.5 cm) of leucocratic material which cross-cut the foliation. These small stringers are commonly less than 10 cm long and are terminated in concordant leucocratic layers at both ends. Commonly, there is no observable difference between the leucocratic layers and the cross-cutting "dikes". These dikes probably represent failure in the relatively competent mesosome, forming cracks which were filled by melt.

Conclusively determining the origin of the cross- cutting "dikes" in the study area, either from the intrusion of the RMS or from local partial melting, is especially difficult. The sills associated with the emplacement of the RMS are granitic. Since low temperature partial melts are also granitic, the difference between dikes originating by these separate processes is not always readily determinable on the basis of simple mineralogy. An additional complexity is the abundance of small sills and dikes, clearly derived from Red Mountain syenite sills, found extending into Bluegrass Creek suite rocks.

Microscopic Evidence

Many rocks contained macroscopic textural evidence of partial melting. However, most convincing were microscopic textures in rocks which in outcrop were uninspiring.

Bimodal Biotite Size and Fabric

In pelitic samples collected close to the contact with the Red Mountain Syenite, the presence of two types of biotite in the same thin section is common. Small (< 2 mm) well-oriented biotite grains are found in regions immediately adjacent to generally coarser-grained regions in which the biotites, though less abundant, are randomly oriented and distinctly larger (Figure 7.2). The larger flakes are found in the leucocratic portion of the rock, especially within the poikilitic rocks described below.

Recent experimental work on biotite nucleation and growth indicates that nucleation of biotite from a silicate liquid is relatively difficult. In experimental runs which produce biotite, a few large grains form instead of many small grains (Peterson, J.W.,1986, pers. comm.). The small oriented biotites are therefore interpreted to record recrystallization in the solid state (part of the mesosome) whereas the large unoriented grains in the leucosome formed by crystallization from a partial melt.

Further from the contact in rocks which contain garnet but no orthopyroxene, rare samples contain; 1) brown biotite defining the foliation and 2) green biotite (rarely with vermicular intergrowths), primarily in the leucosomes.

Vermicular Intergrowths with Biotite

Many of the rocks of the Bluegrass Creek suite contain biotite grains fringed by varying thicknesses of vermicular intergrowths (figure 5.5). Vermicular intergrowths, in particular myrmekite (quartz-feldspar), are known from igneous terrains as well as moderate- to high-grade metamorphic terrains. However, these intergrowths are between biotite and K-feldspar or quartz, and become increasingly common as the contact is approached. This is not inconsistent with the presence of an intergranular melt. Gates (1963, Fig. 8) describes a similar texture from graphic granite in which muscovite-plagioclase intergrowths occur and may provide a low-Fe igneous analog for the textures observed in the BCS.

Biotite Aspect Ratios

Many biotite-rich "restitic" layers and pods (zones from which melt has been extracted, concentrating assemblages with higher melting temperatures) contain very thin flakes of biotite. This is in accord with the results of Dougan (1983), who measured the aspect ratios (length : width) of biotites in pelites from which variable amounts of melt had been removed. He concluded that in rocks from which progressively higher percentages of melt had been extracted, there was a correlative increase in biotite aspect ratio. The high aspect ratios in biotites from pelitic units in the BCS indicate partial melting and removal of unknown quantities of melt.

Poikilitic Texture

In rocks closest to the contact, a poikilitic texture is pervasively developed. The texture is quite striking in thin section (Figure 7.3), however, due to the fine grain size it is not readily apparent in hand sample.

The vast majority of oikocrysts are K-feldspar. However, poikilitic quartz, biotite and cordierite are found in orthopyroxene bearing rocks, perhaps indicating co-crystallization of three or more phases.

K-feldspar oikocrysts contain round inclusions of quartz, cordierite, and less commonly biotite and orthopyroxene. Rare quartz oikocrysts commonly have round inclusions of K-feldspar and cordierite.

Grapes (1985), working on rocks which were partially melted and then chilled during volcanic eruption, described round inclusions of quartz and feldspar in glass that may provide an analog for these oikocrystic textures. If the glassy portions of Grapes' samples had cooled slowly enough, it is likely that the two major mineral phases to crystallize would have been quartz and K-feldspar or plagioclase (based on analyzed glass compositions).

With this in mind, the quartz and K-feldspar oikocrysts might be explained in the following manner. Consider the melting of quartz and K-feldspar in the presence of other minerals (eg. biotite, garnet, cordierite, and/or orthopyroxene) (figure 7.4). If the ratio of K-feldspar to

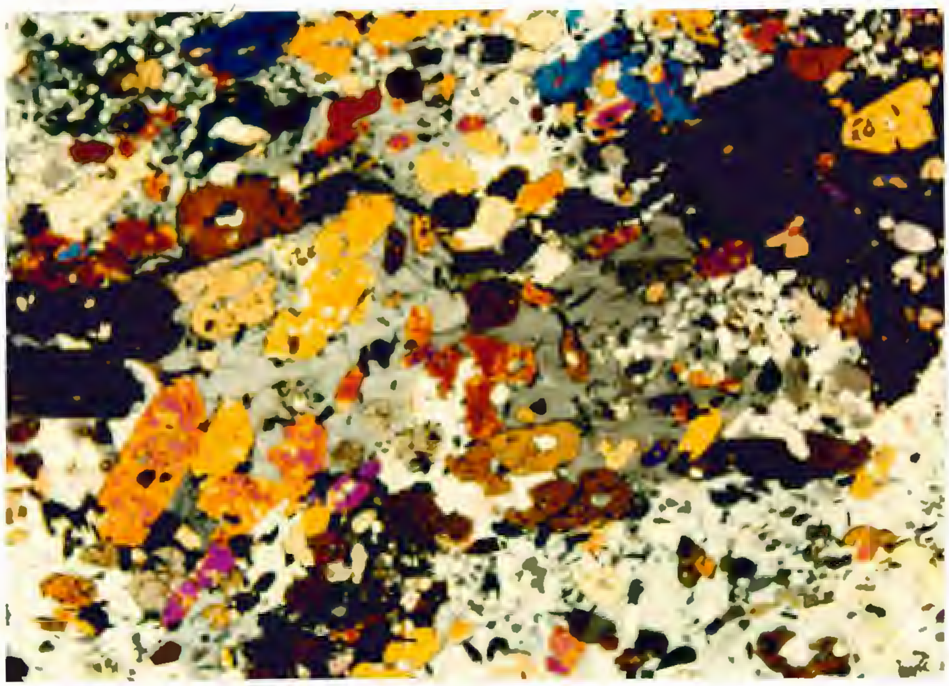

Fig. 7.3. Photomicrograph of poikilitic texture in metapelite. K-feldspar oikocrysts (grey) surround sub- to euhedral orthopyroxene (moderate birefringence), quartz (low birefringence), and graphite (black). Sample SB-7. Crossed polars. Photo is 9 mm across.

quartz in the rock is lower than the ratio of K-feldspar to quartz which is entering the melt, a point will be reached where the supply of K-feldspar is exhausted. Depending on the size of the heat source and the composition of the remaining phases, some undigested quartz may persist. Upon cooling, the recrystallization of the quartz from the melt is facilitated by suspended quartz nuclei. In contrast, the K-feldspar nuclei are absent and crystallization is delayed. Once a K-feldspar nucleus forms, it may grow rapidly and form a large oikocryst.

Orthopyroxene, a common phase in samples containing the poikilitic texture, shows a wide range in grain size. However, it rarely includes any other minerals, suggesting that orthopyroxene is a phase which crystallized relatively early in the partial melting process (e.g. during incongruent melting) and/or early in the crystallization of the melt. Biotite which rims orthopyroxene may represent reequilibration in the presence of a liquid in response to new conditions (e.g. an increasingly hydrated liquid composition) during crystallization of the derived melt. A possible reaction might be:

Orthopyroxene + melt = Biotite ± K-feldspar ± Qtz

Igneous Plagioclase

Locally, elongate laths of plagioclase (Figure 4.5) occur in rocks with the poikilitic texture. These laths do

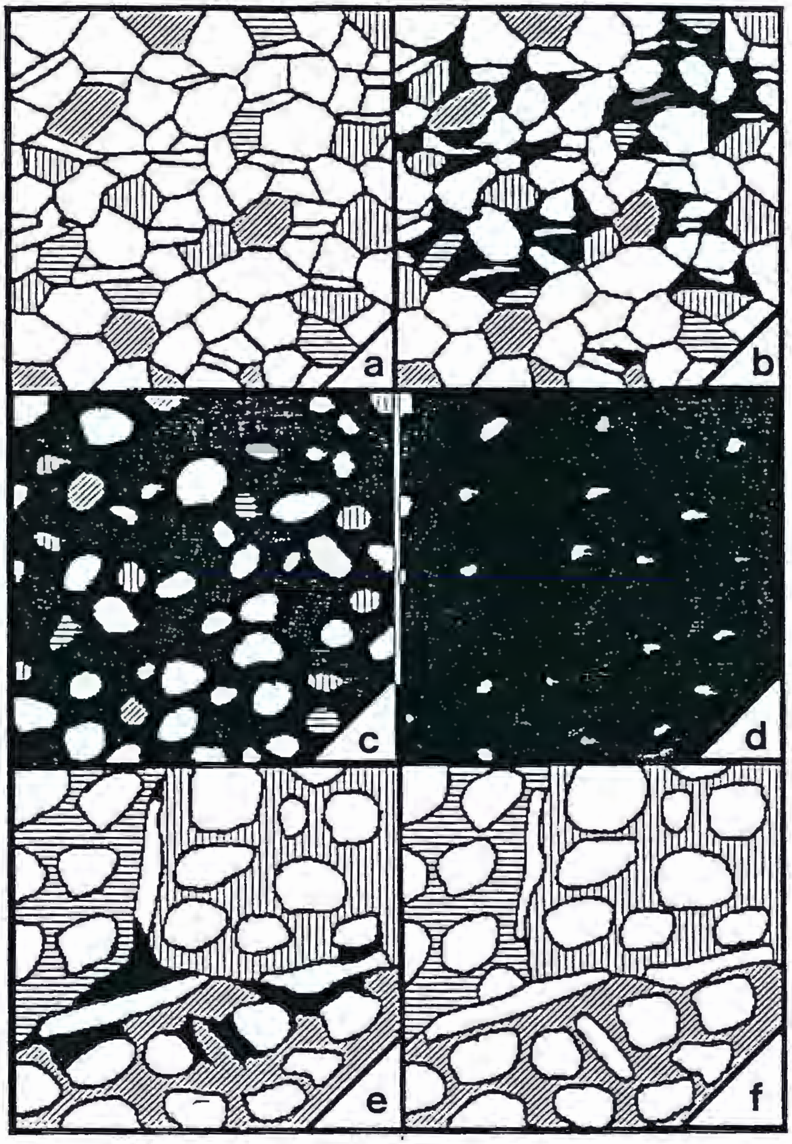

Fig. 7.4. Speculative process for the development of poikilitic textures in metapelites by partial melting. Biotite is brown, K-feldspar is striped, quartz is white, and melt is black. Other phases are excluded for simplicity. Starting with mildly foliated gneiss (a), increasing temperature results in melting at triple-junctions where three different phases are in mutual contact (b). As melting proceeds, biotites initially show an increase in aspect ratio and eventually may be consumed (C). Further melting encorporates quartz and K-feldspar in appropriate ratio until only quartz remains as a solid phase (D). Increasing temperature may allow remaining quartz to melt (not shown). Upon cooling, K-feldspar growth is inhibited by slow nucleation rates relative to quartz, and the poikilitic texture results(e,f).

not look like metamorphic plagioclase and probably crystallized from a partial melt.

Orthopyroxene Overgrowths

In the large xenolith in the Red Mountain Syenite south of Tunnel Road (Plate 1), rare orthopyroxene grains appear to have optically continuous overgrowths (figure 7.5). The overgrown orthopyroxene appears to be subhedral with at least one crystallographically determined face. The overgrowth indicates at least two distinct episodes of orthopyroxene growth (e.g. growth by incongruent melting reactions followed by direct crystallization upon cooling at reduced $X(H_2O)$.

Terminated Quartz and "Graphic Intergrowths"

One sample of pelitic migmatite, from the same xenolith south of Tunnel road, displays terminated quartz crystals projecting into K-feldspar (Figure 7.6). These quartz grains are in optical continuity and have evidently nucleated on earlier quartz. Since quartz has such a low anisotropy of surface energy, the good terminations imply that the quartz grew into a fluid. The question remaining is whether the fluid was a vapor or a silicate melt.

The feldspar surrounding the terminations is a single crystal intergrown with the quartz, not unlike graphic granite. This sample also contains abundant oikocrysts of

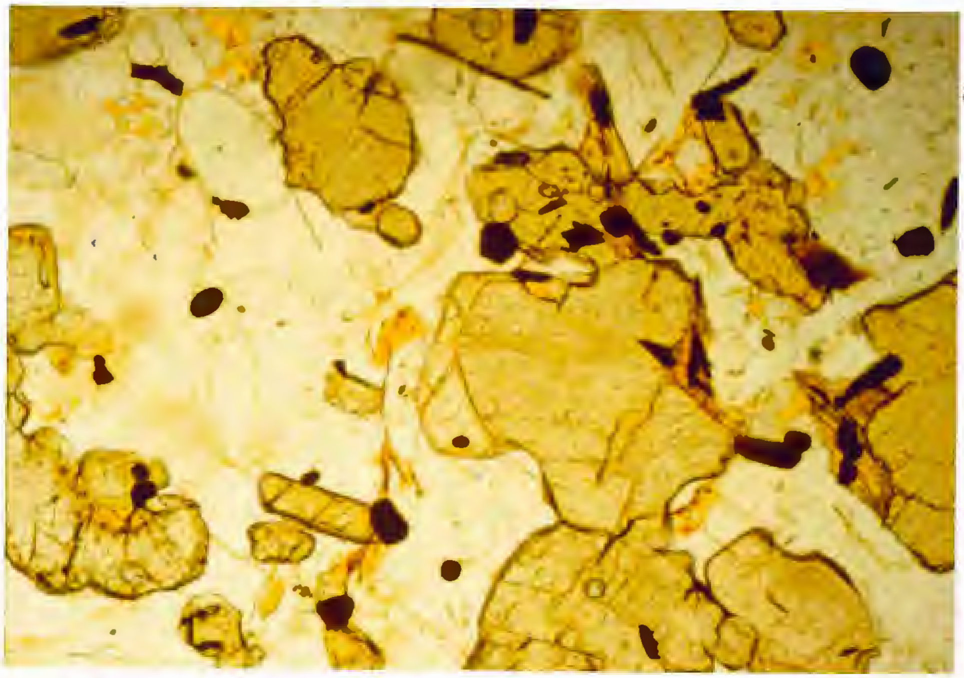

Fig. 7.5. Photomicrograph showing optically continuous orthopyroxene overgrowth. Matrix is K-feldspar, quartz, cordierite (all low relief), and graphite (black). Sample SB-3. Plane light. Photo is 3.5 mm across.

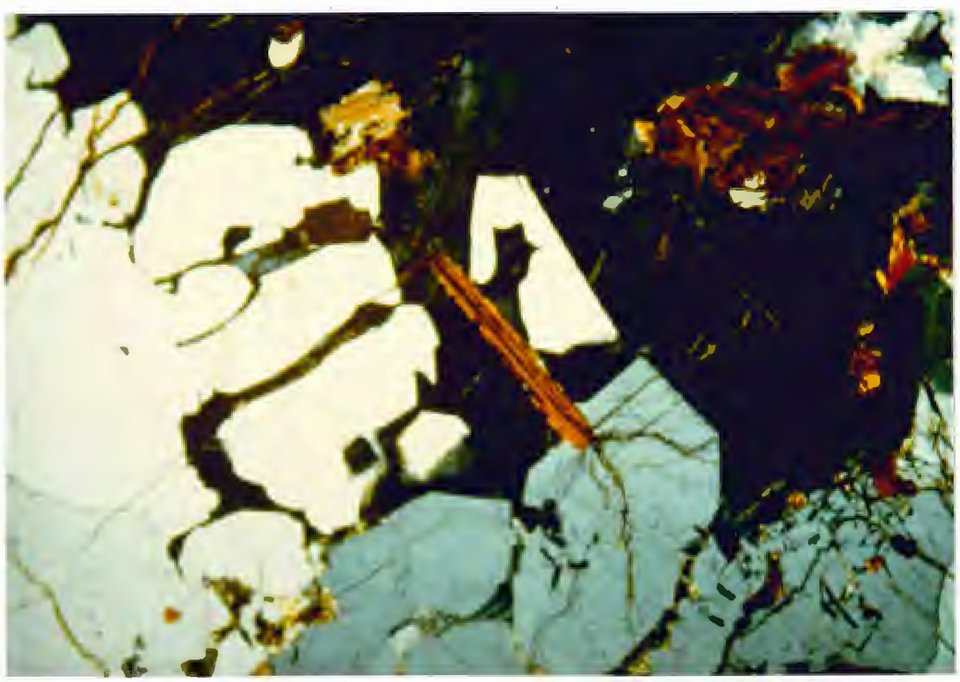

Fig. 7.6. Photomicrograph of terminated quartz grains (white and grey) in a micrographic intergrowth with K-feldspar (at extinction). Note large euhedral biotite (brown). Sample SB-8. Plane light. Photo is 9 mm across.

K-feldspar, quartz, and biotite. It is inferred from these relations that the terminated quartz grains grew into a silicate liquid with a composition similar to those which produce graphic granite. That is, they were crystallized from "granitic minimum" melts derived from the pelitic rock in which they are found.

Leucosomes

Leucosomes in the area generally contain abundant quartz and feldspar. In these leucosomes, many of the minerals tend to be euhedral (e.g., cordierite, plagioclase, biotite, garnet, orthopyroxene and rarely quartz). They are generally much coarser than their counterparts in the mesosomes but are gradational in size with them.

The poikilitic texture in the orthopyroxene-bearing leucosomes helps constrain the order of crystallization process, with orthopyroxene forming first, either as a product of incongruent melting or an early crystallized phase, followed by the crystallization of cordierite, biotite, quartz, K-feldspar, (possibly at a eutectic). The K-feldspar oikocrysts may owe their existence to difficulties in nucleating K-feldspar in melts with high Fe and Al contents, where early biotite and cordierite crystallization would be favored.

Restites

In general, restites contain the Fe, Mg, and Al-rich minerals which cannot be incorporated into the liquid. High concentrations of the assemblages in restites include; 1) garnet with biotite ± cordierite; 2) orthopyroxene and cordierite, with lesser amounts of biotite and spinel; and 3) garnet, magnetite and quartz with traces of biotite. The ferromagnesian minerals show a wide variety of morphologies. Locally anhedral mafic phases are intergrown with quartz or feldspar, but not both (eg. garnet-quartz- magnetite intergrowths). In other zones, mafic phases appear as subhedral grains and rarely as euhedral grains.

The restites identified as such in the field were restricted to garnetiferous varieties. The orthopyroxene restites are finer-grained so their restitic nature was not obvious in hand samples. Restites are typically only a small percentage of the rock. The thickest recognized resititic layer (2 cm) is >80% garnet, with euhedral garnets 1-2 cm in diameter. Restites locally have low- temperature melting assemblages trapped in the interstices (e.g. Qtz-Kfs-Bio).

Low-Temperature Melting Compositions and the BCS

There are two common rock compositions which melt at relatively low temperatures. The best known is the "wet granite" which melts at about 650°C at 3 kb (Figure 2.1)

(Tuttle & Bowen, 1958). However, quite a range of pelitic compositions can also begin to melt within a few tens of degrees of this reaction (eg. Grant, 1985, figure 3.16).

Partial melts of pelitic rocks are peraluminous. S-type granites are corundum normative and crystallize from peraluminous magmas (Clark, 1981). S-type granites formed by partial melting of felsic crustal rocks, as opposed to fractional crystallization of a basaltic melt, according to evidence from major element (e.g. Currie and Pajorie, 1981; Strong and Hanmer, 1981), trace element (including REE) (e.g. Goad and Cerny, 1981), and isotopic studies (e.g. Halliday, Stephens, and Harmon, 1981).

Cordierite can be an important phase in low-temperature melting compositions. It occurs as a primary igneous phase in granites (e.g. Phillips, Wall, & Clemens, 1981). However, it is also a commonly a phase in low- to moderate- pressure metamorphic rocks. The change from anhedral to subhedral and euhedral morphologies toward the RMS contact may be evidence for the two different origins.

Garnet is also a common phase in peraluminous igneous rocks. Many of the leucosomes in the Bluegrass Creek suite contain abundant garnet. There are three possibilities for this common association: 1) all the garnet crystallized directly from the melt (this seems unreasonable as the concentration of garnet is much too high in many cases for a reasonable partial melt composition), 2) significant amounts of garnet existed prior to melting and were concentrated as partial melts migrated out of the rocks, leaving behind the refractory garnets, 3) the garnets were a product of incongruent melting (see the biotite-absent reaction, figure 7.8).

Partial-Melting Reactions

The determination of partial-melting reactions from textural and mineralogical data is difficult. The leucosome composition, the adequate chemical system for modeling, the interpretation of which minerals crystallized from the melt and which were products of incongruent melting are all subjects which require careful observations and many judicious assumptions. This section presents a set of reactions consistent with the textural and mineralogical relations as observed in outcrop and thin section, as well as with the pertinent published experimental data.

The two assemblages most common in the leucosomes are the garnet-bearing assemblage Qtz-Kfs-Pfs-Bio-Cdt-Gar and the orthopyroxene-bearing assemblage Qtz-Kfs-Pfs-Bio-Cdt-Opx. The simplest system needed to fully explain these equilibria would be CNKFMASH ($CaO-Na_2O-K_2O-FeO-MgO-Al_2O_3-SiO_2-H_2O$).

In order to simplify the system a few assumptions can be made. First, since plagioclase is usually minor or absent in the leucosomes, it will be not considered in the phase relations. The system can then be modeled in KFMASH with the important phases being Qtz-Kfs-Bio-Cdt-Gar-Opx.

Quartz is nearly ubiquitous in the leucosomes and is assumed to be in excess in all rocks considered in this section. The major mineralogical relations can be plotted schematically in a pseudo-AKFM tetrahedron and projected onto the AFM plane from K-feldspar, as in figure 7.7. Mineral compositions are taken from similar rocks in the Morton Pass area, after Grant (1985b, fig. 12). Variation in individual mineral species composition is expected with changing conditions, however, as a first approximation, they may be represented as points. Petrographic evidence suggests that the liquid compositions lie within the Gar-Bio-Cdt and the Opx-Bio-Cdt fields, and the projection shows the field for silicate liquids compatible with these observations.

The possibility for two or more chemically distinct liquids (from two different original bulk compositions) occurring in adjacent areas which are not communicating (they are not connected by pores) should not be ignored, as this appears to be possible in subsystems of KFMASH (see Levin, Robbins, & McMurdie, 1966). These liquids would not be immiscible, but two chemically distinct melts at the same temperatures.

Following Grant (1985b) (using a different melt composition) and assuming a binary vapor to be present and

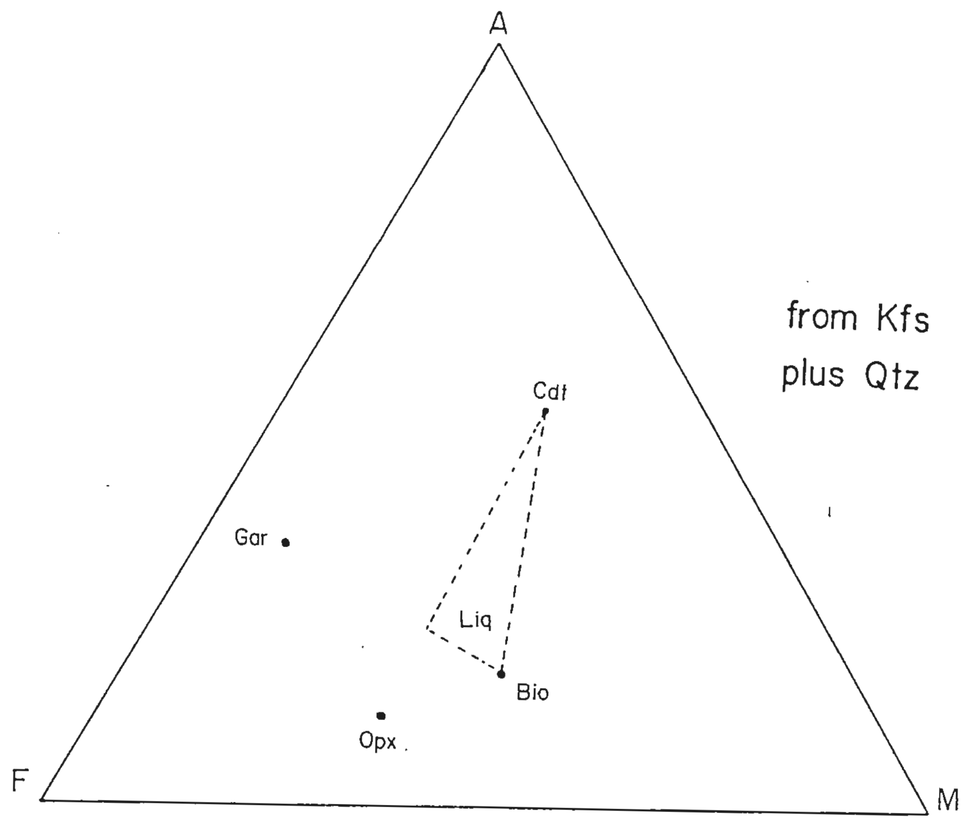

Fig. 7.7. Plot of AFM mineral compositions from Grant (1985) projected from K-fledspar, assuming excess quartz. Also shown is a probable field for the composition of a coexisting melt, as deduced from inferred liquidus relation in the Bluegrass Creek Suite (this liquid composition is different than in Grant, 1985).

using Schreinemakers analysis, the reactions about the Mus-Als-absent invariant point are shown in T-X(H_2O) space (figure 7.8). The melt-producing reactions below the isobarically-invariant point in T-X(H_2O) space are, with increasing temperature:

Qtz + Kfs + Bio + Cdt + Gar + Vap = Liq (Opx)

Qtz + Kfs + Bio + Gar + Vap = Opx + Liq (Cdt)

Qtz + Bio + Gar + Vap = Cdt + Opx + Liq (Kfs)

Qtz + Bio + Gar = Kfs + Cdt + Opx + Liq (Vap)

(see Figure 7.8). The first 3 reactions occur in the presence of a vapor, while the last reaction, involving the breakdown of biotite and garnet in the presence of quartz does not involve vapor. Note that if equilibrium is maintained, the "vapor- absent" reaction can only occur at the invariant point, if the second component of the vapor does not enter the liquid ($f = 6 + 2 - 7$; P = constant)

The melt-producing reactions at temperatures higher than at the invariant point are:

Qtz + Kfs + Bio + Cdt + Opx + Vap = Liq (Gar)

Qtz + Kfs + Cdt + Opx + Vap = Gar + Liq (Bio)

Kfs + Cdt + Opx + Vap = Bio + Gar + Liq (Qtz)

The activity of water in the system before, during and after melting is thus an important consideration. Before melting, the activity of H_2O was probably low because; 1) the supracrustals had undergone a previous high-grade regional metamorphism, 2) the heat source, the Red Mountain

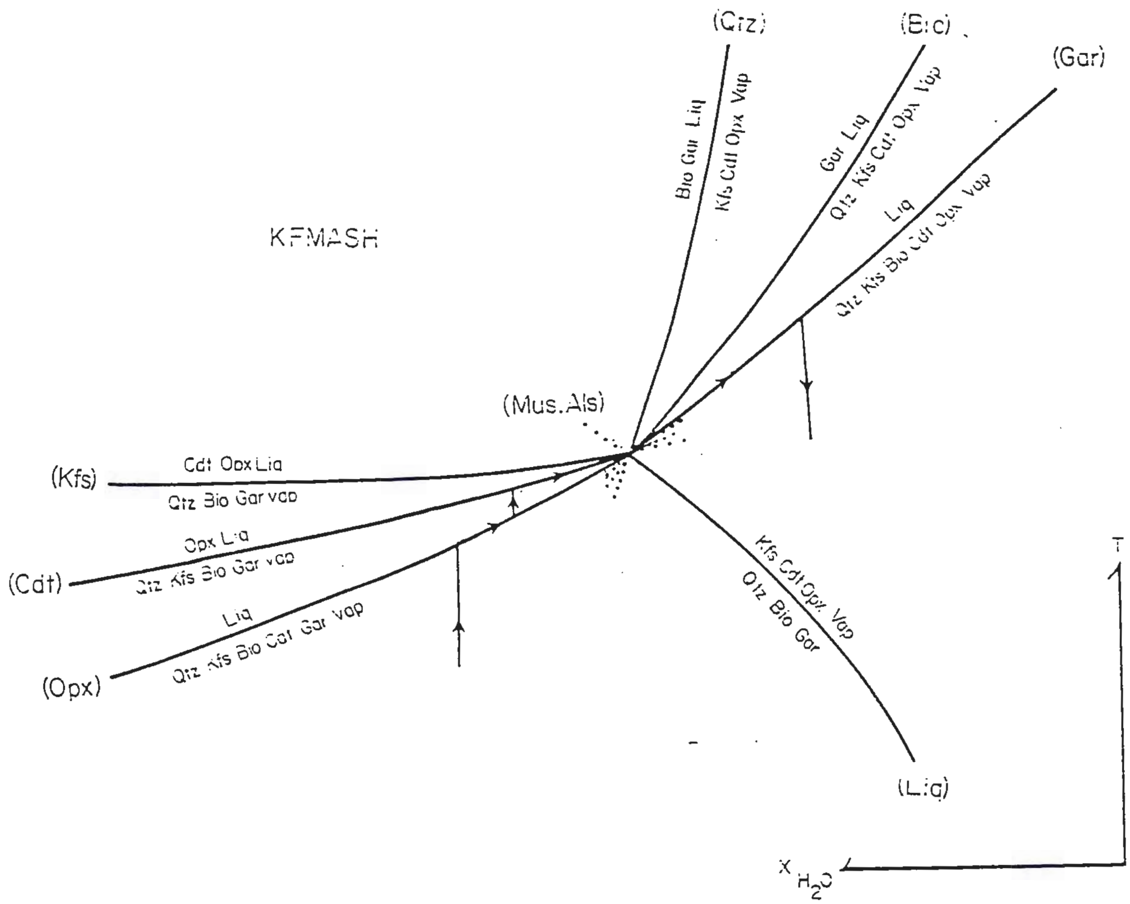

Fig. 7.8. Schreinemakers' analysis for the system KFMASH. Relations consistent with observed petrogenesis are plotted in T-$X_{(H_2O)}$ space. The aluminosilicate-muscovite absent invariant point is modified after Grant, 1985 (fig. 3.14). The arrows indicate one possible path to explain orthopyroxene bearing migmatites. Early congruent melting buffers the composition of the coexisting vapor until cordierite is eliminated. After an increase in temperature, incongruent melting produces orthopyroxene and liquid while buffering the system towards the invariant point, where the vapor absent incongruent melting reaction Qtz + Bio + Gar = Kfs +Cdt + Opx + Liq occurs. With increasing temperature, the reaction again becomes congruent. As the system cools, it crystallizes Qtz-Kfs-Bio-Cdt-Opx at a eutectic.

Syenite, probably did not evolved significant quantities of H_2O, and 3) the production of CO_2 from decarbonation reactions in adjacent units acted as a dilutant to the metamorphic fluid.

The initial melting probably was vapor-present, and the congruent melting reaction (the (Opx) reaction, figure 7.8) at relatively high $X(H_2O)$ is favored as it could explain the absence of cordierite (limiting reactant) and the presence of garnet in the lowest temperature leucosomes. Assuming the vapor was buffered by the reactions occurring in the rocks, the first three reactions would all drive the system towards the invariant point. As melting proceeded, the activity of H_2O would be reduced because H_2O is more soluble in silicate liquids than is CO_2. The composition of the vapor would be buffered along the melt producing curves towards the invariant point.

At the invariant point, the vapor-absent reaction then becomes an important melting reaction, as it does not require the participation of a vapor phase. If garnet is taken as the limiting reactant, the residual system would contain Qtz-Kfs-Bio-Cdt-Opx-Liq, which is the essence of the leucosomes nearest the contact. This reaction may explain the paucity of coexisting garnet and orthopyroxene.

Applying the schematic grid (figure 7.8), some conclusions may be drawn. It is clear that if the garnet-bearing leucosomes represent partial melts, then they equilibrated on the high $X(H_2O)$ side of the invariant point (otherwise they would bear orthopyroxene). Similarly, orthopyroxene-bearing leucosomes equilibrated on the low-$X(H_2O)$ side of the invariant point. Higher temperatures for the formation of orthopyroxene bearing rocks may also be inferred.

Crystallization and Liquidus Reactions in the Melts

The textural and mineralogical relationships in the leucosomes, particularly those with orthopyroxene, indicate the crystallization of the partial melts. To determine the liquidus versus the solidus phases, igneous textures can be used to work out the crystallization path (e.g. inclusions, morphologies, etc.). The interpretation is made less than certain by the potential for very different and changing liquid compositions.

The garnet-bearing leucosomes can only be explained in the present model by crystallization on the high $X(H_2O)$ side of the muscovite-sillimanite absent invariant point (figure 7.8, 7.9a). The orthopyroxene absent reaction (congruent melting) produces the appropriate assemblage found in garnet-bearing leucosomes.

The model for the orthopyroxene-bearing leucosomes starts with crystallization of orthopyroxene by incongruent melting and/or crystallization directly from the melt (figure 7.8,7.9b). Then cordierite or biotite joins in along a

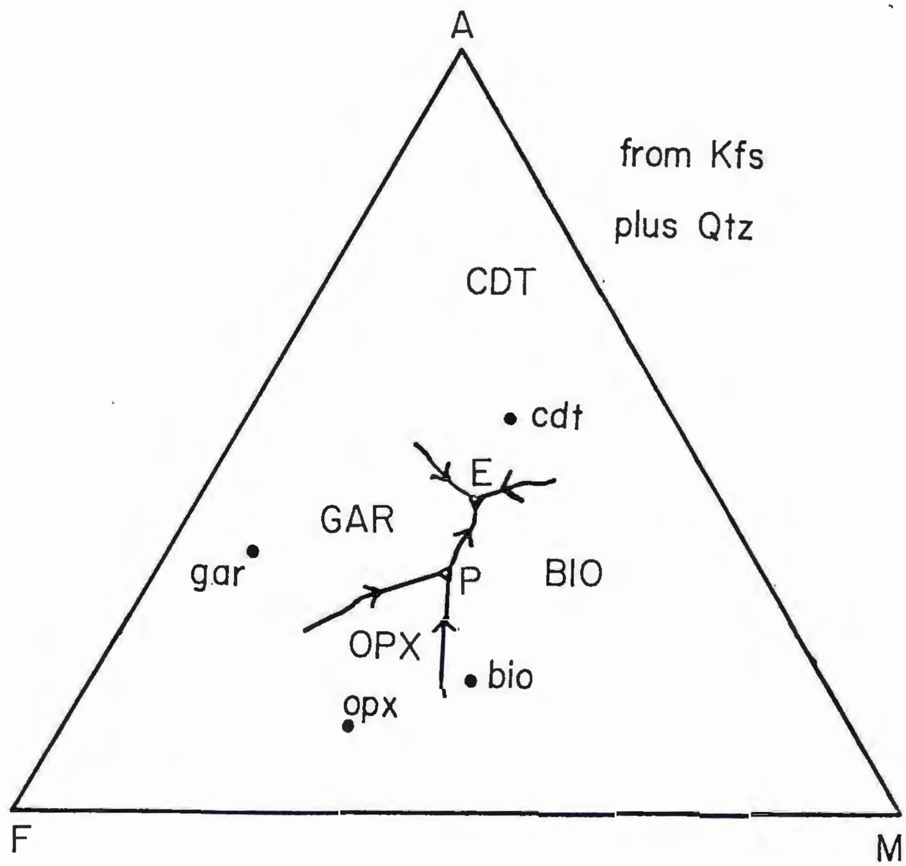

Fig. 7.9a. Highly schematic isobaric liquidus diagram at constant X(H_2O) (higher than the muscovite-sillimanite absent invariant point of figure 7.8). Relations projected from K-feldspar assuming excess quartz. Lower case indicates approximate composition (from Grant, 1985), capitol letters indicate fields of crystallization. Open triangle (P) is peritectic reaction point which corresponds to the cordierite absent reaction (figure 7.8). Closed triangle (E) is the eutectic point (orthopyroxene absent reaction).

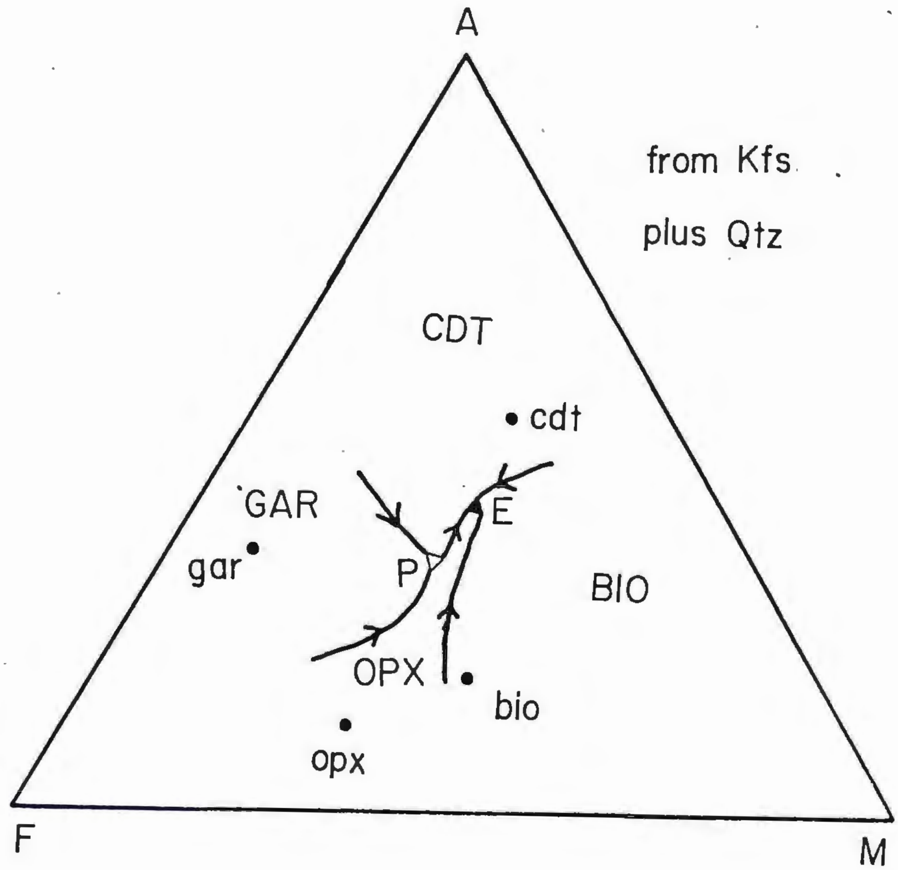

Fig. 7.9b. Highly schematic isobaric liquidus diagram at constant X(H_2O) (lower than the muscovite-sillimanite absent invariant point of figure 7.8). Relations projected from K-feldspar assuming excess quartz. Lower case indicates approximate composition (from Grant, 1985), capital letters indicate field of crystallization. Open triangle (P) is peritectic reaction point which corresponds to the biotite absent reaction (figure 7.8). Closed triangle (E) is the eutectic point (garnet absent reaction).

cotectic. At the eutectic (E), quartz, K-feldspar, cordierite, biotite, and orthopyroxene all crystallize. The vermicular intergrowths of biotite with K-feldspar and orthopyroxene are consistent with the proposed eutectic.

CHAPTER 8: CONCLUSIONS

The rocks of the Bluegrass Creek suite were affected by at least two major metamorphic events. The first, a regional metamorphism during the Archean (about 2.6 b.y.), involved temperatures in excess of 550°C and pressures near 6 kb during a large-scale regional event. The amphibolite facies event significantly dehydrated the BCS, setting the stage for partial melting.

The second metamorphic event, due to the intrusion of the Laramie Anorthosite Complex at 1.4 b.y., took place at lower pressures (3 kb) and resulted in higher temperatures close to the contact (>800°C). The complex was emplaced in at least two major pulses. The first formed a large (200 km^2) anorthositic body (1100°C at intrusion), whereas the second involved smaller volumes of syenitic magma intruded along the margins of the anorthosite at temperatures in excess of 900°C. This double pulse of thermal energy into the previously metamorphosed BCS resulted in partial melting of pelitic compositions.

A series of isograds was mapped in the BCS (plate 2) in an area along the northern contact of the Red Mountain syenite (the local source of the second pulse of thermal energy). In rocks furthest from the contact, the lowest-grade assemblage contains Kfs-Als-Gar (zone 1 or 2, figure 5.1). Toward the contact, the successive zones encountered are characterized by the appearance of the new mineral assemblages Kfs-Cdt-Spl (zone 4), Kfs-Cdt-Gar (zone 5), Kfs-Cdt-Cor-Spl (zone 6), Kfs-Cdt-Opx (zone 7), and in a xenolith within the syenite, Kfs-Opx-Spl (zone 8).

The single mappable isograd in the marbles, the tremolite-out isograd, occurs between the Cor isograd and the Kfs-Cdt-Opx isograd in the pelitic rocks. Together, these relations imply increasing temperature and a lowering of the activity of water toward the contact (figure 5.1).

Evidence of partial melting is best preserved in orthopyroxene-bearing rocks. The abundance of textural and mineralogical evidence presented indicates significant volumes of melt (perhaps as much as 50% of the original rock volume) were produced locally. Comparison with experimental work, consideration of theoretical data, field relations and petrologic observations suggest that partial melting near the contact of the Red Mountain Syenite may best be explained utilizing figures 7.8, 7.9a, and 7.9b.

Textures consistent with partial melting within the pelites include: extensive and pervasive segregation; disrupted foliation; bimodal biotite grain size and fabric; vermicular intergrowths of biotite with quartz and K-feldspar; free growth of quartz; K-feldspar and quartz oikocrysts; orthopyroxene overgrowths; igneous-appearing plagioclase; and euhedral cordierite, biotite, and orthopyroxene.

Orthopyroxene occurs in leucosomes closest to the contact and importantly, garnet is absent. Further from the contact orthopyroxene is absent, whereas garnet is abundant. The mapped distribution of assemblages record a decrease in the activity of H_2O and an increase in temperature toward the contact (see figure 7.8). These findings indicate that the Red Mountain syenite, though a source of heat, was not an important source of H_2O. In fact, the RMS may have acted as a sink for H_2O which evolved early in the contact metamorphism by dehydration reactions in the adjacent BCS.

This study demonstrates that the high-grade metamorphism associated with the intrusion of the Laramie Anorthosite complex resulted in the partial melting of pelitic rocks in the Bluegrass Creek suite. Theoretical melting reactions proposed are consistent with all the available data and confirm the viability of this process. The evidence of partial melting in high-grade metamorphic terrains is commonly obscured by later deformation. However, in the Bluegrass Creek suite, due to the lack of later deformation, primary igneous textures are preserved in pelitic migmatites. This unique opportunity to assess partial melting mechanisms in natural sedimentary rocks provides important constraints for the genesis of peraluminous granites.

APPENDIX 1

ABBREVIATIONS

A	Aluminosilicate
a	Apatite
Als	Aluminosilicate
And	Andalusite
B	Biotite
BCS	Bluegrass Creek Suite
Bio	Biotite
C	Cordierite
c	Chlorite
Cc	Calcite
Cdt	Cordierite
Cor	Corundum
czo	Clinozoisite
D	Diopside
Dio	Diopside
Dol	Dolomite
For	Forsterite
G	Garnet
g	Graphite
Gar	Garnet
H	Hercynite (Spinel)
h	Hornblende
hbd	Hornblende
i	Ilmenite
Kya	Kyanite
LAC	Laramie Anorthosite Complex
M	Muscovite
Mus	Muscovite
mag	Magnetite
O	Orthopyroxene
Ol	Olivine
Opx	Orthopyroxene
P	Plagioclase
Pfs	Plagioclase
Phl	Phlogopite
Q	Quartz
Qtz	Quartz
R	Corundum
r	Rutile
RMS	Red Mountain Syenite
Sca	Scapolite
Srp	Serpentine
Sil	Sillimanite
SMG	Squaw Mountain Granite
Sph	Spene
Spl	Spinel
Sta	Staurolite
Tre	Tremolite
t	Tourmaline
X	Opaques
z	Zircon

APPENDIX 2

MINERALOGY AND EQUILIBRIA FOR PELITIC AND QUARTZOFELDSPATHIC ROCKS

SAMPLE d	MINERALS PRESENT	INFERRED EQUILIBRIA
SB-1	QKPMBCX aigmz	QKBC
SB-3	QKPBCHOX agz	KBCHO, QKBCO
SB-4	QKBCHOX gz	QKBCO
SB-6	QKBC z	QKBC
SB-7	QKBCOX giz	QKBCO
SB-8	QKPBCHOX g	QKBCO, KBCH
SB-10	QKPBCHOX giz	KBCH, QKBCO
SM1-1	QKMBRHX rz	QKPB
SM3-1	QKPB z, allanite RMS	QKPB
SM3-2	QKPBC z	QKPBC
SM4-1	QKPBCH z	QKPBC
SM4-3	QKPMBCGX crz	QKPBCG
SM4-3A	QKPMB	QKKPB
SS5-3	QKPMBX z	QKPB
SS5-5	QKPB	QKPB
SS6-1	MBGHX z	MBGH
SS6-1A	QKPMB	QKPB
SS6-2	QKPMBGX c	QKPBG
SS6-2A	QKABCHX tz	QKBC, BCH
SS6-3	QMPABGH z	QPAB, ABH
SS6-7	QKB chrz dike rock	QKB
SS7-1	QKPB cz, allanite	QKPB
SS7-3	QKPMB	QKPB
SS8-1	QKPMABCX z	QKABC
SS9-1	QKPMABGHX rz	QKPB, QPBH, QBGH
SS9-2	KMABGHX z	KABGH
SM9-4	QKPMBCG	QKBC, QKBG
SS13-1	QKABCX arz	QKBC, KABC
SS13-2	QKPMB	QKPB
SS13-3	KABH	KABH
SS13-4	KABCHX z	KABC, ABCH
SS13-5	QKBGX z	QKBG
SS13-6	QBCGHX z	QBGH, BCGH
SS13-7	QKBCHX z	QKBC, QKAH
SS13-8	KABCX m	KABC
SS13-9	QKBX z	QKB
SS13-10	QKABCH	QKB, KABC, ACH
SS15-1	QKPB	QKBC
SS16-1	QKPBX z	QKPB
SS16-1A	QBCX m	QBC
SS16-3	QBCX z	QBC
SS16-4	QKABCH	QKBC, KABC, ACH
SM17-1	QKPB	QKPB
SS18-1	QKMB	QKB
SM19-1	QPBCGH t	QPBCG, PBCH
SM20-1	QKBX	QKB

SAMPLE d	MINERALS PRESENT	INFERRED EQUILIBRIA
SM20-3	QKB hz, allanite RMS	QKB-hbd
SM20-4	QKBGX z	QKBG
SM20-6	QKPBGOX z	QKBG, QKBO
SM21-2	QKMABCX	QKBC, ABC
SM22-2	KPABCRX cr	KABR, KABC
SM24-1	QKABRX rz	QKB, KABR
SM24-2	QKAB r	QKAB
SM27-1	QKPMB mylonite	QKPB
SM28-1	QKPABCHX z	QKBC, KABC, CH
SM28-2	QKPABCGHX z	QKBCG, KABCH
SM29-1	QKPMABCH	QKPBC, KPABC, PBAH
SM29-2	QPBCGHX z	QPBCG
SM31-1	KPABHRX	KPABH, KBHR
SM31-1A	QKPB z granophyre	QKPB
SM31-2	QKPBC z	QKPBC
SM31-3	KABCHX	KABC, ABCH
SS32-4	QKPBCH rz	QKB, QBC
SS34-3	QKABC tz	QKBC, AC
SS34-4A	QKPBCG z allanite	QKPBG, KPBC
SB34-4B	QKPBX z	QKPB
SS34-7	QKABCGHX z	QKBG, QKACH, QKBC
SM35-1	KABCHX rz	KACH, KBCH
SM35-4	QKPABCHX airz	QKPBC, KABCH
SM35-8	QKBCX z	QKBC
SM35-9	KABCHX rz	KACHR, KAB
SS36-1	QKMABC	QKBC
SS36-1	QKPMB	QKPB
SS37-1	QKPB	QKPB
SS37-2	QKPB	QKPB
SM40-5	QKABCX	QKAC, KABC

APPENDIX 3

MINERALOGY OF "OTHER" ROCK TYPES

SAMPLE	MINERALS PRESENT
SB-2	Cc-Srp-Phl-X
SB-7	Cc-czo-Dio-Sph-Tre
SM4-4	Qtz-Pfs-Tre-Bio-chl
SM4-5	Cc-Srp-Dio
SS-4	Cc-Tre-czo-
SS7-2	Cc-Tre
SS7-5	Qtz-Hbd-Pfs-az
SS10-1	QKPB-Dio-Hbd-chl-z
SS16-2	Pfss-Tre-Sph-Phl-gx
SS17-3	QPX-Hbd
SM22-1	Cc-Srp-czo-Phl
SM25-1	Sph-Dio-Phl-Tre
SM25-2	QPB-Hbd
SM27-2	Cc-Phl-Srp-For
SM28-3	Cc-Tre-czo-X
SM28-4	Pfs-Spl-X-Hbd
SM30-1	Cc-For-Srp-X
SM30-2	Cc-For-Srp-Spl
SS32-1	QPBGX-Hbd-chl-Mus
SS32-2	Cc-Srp-For-Spl-X
SS33-1	Cc-Srp-Dop-X
SS32-4	QKPBz-Hbd
SS34-2	QKB-Hbd-a-z
SS34-5	Cc-Pfs-For-Phl-X-Srp
SS34-6	Cc-For-Srp-Sph-Spl-Phl
SM35-2	Pfs-Dio-Hbd-X
SS35-3	QPBX-Hbd
SS35-5	Bio-Phl-Sph-Sca-Dio
SM37-3	Cc-Qtz-Pfs-Hbd-chl
Inc-3	Sca-Sph-Dio-g

BIBLIOGRAPHY

Bhattacharya, A., 1986, Some geobarometers involving cordierite in the FeO-Al_2O_3-SiO2 ($\pm H_2O$) system: refinements, thermodynamic calibration, and applicability in granulite facies rocks. Contrib. Mineral. Petrol., 94, 387-394.

Birch, F. and Clark, H., 19??, The thermal conductivity of rocks and its dependance upon temperature and composition. Am. Jour. Sci., 238, 529-558, 613-635.

Bochenski, P., 1982, Contact Metamorphism in the Morton Pass area, Unpubl. M.S. thesis, Univ. Wyoming, 56 p.

Bohlen, S.R., Boettcher, A.L., Wall, V.J., and Clemens, J.D., 1983, Stability of phlogopite - quartz and sanidine - quartz: a model for melting in the lower crust, Contrib. Mineral. Petrol., 83, 270-277.

Bothner, W.A. Jr., 1967, Petrology, structuralgeometry, and economic geology - The Cooney Hills, Platte County, Wyoming, Unpubl. thesis, Univ Wyoming, 164 p.

Busch, W., Schneider, G., and Mehnert, K.R., 1974. Initial melting at grain boundaries. Part II: Melting in rocks of granodioritic, quartzdioritic, and tonalitic composition. N. Jb. Miner. Mh. 1974, 345-70.

Chaterjee, N.D., and Johannes, W., 1974. Thermal stability and standard thermodynamic properties of synthetic $2M_1$ muscovite. Contrib. Mineral. Petrol. 48, 89-114.

Clemens, J.D., and Wall, V.J., 1981, Origin and crystallization of some peraluminous (S-type) granitic magmas, Can. Mineral., v.19, 111-132.

Currie, K.L., and Pajari, G.E. Jr., 1981, Anatectic peraluminous granites from the Carmanville area, Can. Mineral., v.19, 147-162.

Darton, N.H., Blackwelder, E. and Siebenthal, C.E., 1910, Description of the Laramie-Sherman, Wyoming, quadrangles: U.S. Geol. Survey Atlas, Folio 173, 17 p.

Devore, G.W., 1948, Range of composition of orthopyroxene and olivine minerals in the Laramie Range of Wyoming (abs.), Geol. Soc. Amer. Bull., v. 59, p. 1398-1399.

Dougan, T.W., 1983, Textural relations in melanosomes of selected specimens of migmatitic pelitic schists: Implications for leucosome-generating processes. Contrib. Miner. Petrol., 83, 82-98.

Duebendorfer, E.M. and Houston, R.S., 1987, Proterozoic accretionary tectonics at the southern margin of the Archean Wyoming craton. Geol. Soc. Amer. Bull., v. 98, p. 554-568.

Evans, B.W. and Guidotti, C.V., 1966, The sillimanite - potash feldspar isograd in western Maine, U.S.A.. Contr. Mineral. Petrol., v. 12, p. 25-62.

Ferry, D., and Speer, S.A., 1978, Experimental calibration of the partitioning of Fe and Mg between biotite and garnet. Carnegie Inst. Wash., Yearb. No. 76, p. 579-581.

Fowler, K.S., 1930, The anorthosite of the Laramie Mountains, Wyoming, Am. Jour. Sci., v. 219, p. 373-405.

Frost, B.R., 1979, Mineral equilibria involving mixed volatiles in a C - O - H fluid phase: the stability of graphite and siderite. Amer. Jour. Sci., v. 279, p. 1033-1059.

Furham, M.L., Frost, B.R., and Lindsley, D.H., 1988, Crystallization conditions of the Sybille Monzosyenite, Laramie Anorthosite Complex, Wyoming: Jour. Petrol., v. 29, p. 699-729.

Gates, R.M., and Sheerer, P.E., 1963, The petrology of the Nonewaug granite, Connecticut, Am. Mineral., v.48, p. 1040-1069.

Goad, B.E. and Cerny, P., 1981, Peraluminous granites and their pegmatite aureoles in the Winnepeg River district, southeastern Manitoba, Can. Mineral., v.19, 177-195.

Grant, J.A., 1985a, Phase equilibria in low-pressure partial melting of pelitic rocks. Amer. Jour. Sci., v. 285, 409-435.

____________, 1985b, Phase equilibria in partial melting of pelitic rocks, in Migmatites, ed. Ashworth, J.R., Blackie and Son, Glasgow, p. 86-144.

Grant, J.A., and Frost, B.R., 1986, Decompression, melting, and metamorphism in the aureole of the Laramie Anorthosite Complex (abs.), Geol. Soc. Amer. Bull.

Graff, P.J., Sears, J.W., Holden, G.S., and Hausel, W.D., 1982, Geology of the Elmers Rock greenstone belt, Laramie Range, Wyoming. The Geological Survey of Wyoming, Rep. Investigations d 14, 23 p..

Grapes, R.H., 1986, Melting and thermal reconstitution of pelitic xenoliths, Wehr volcano, East Eiffel, West Germany, Jour. Petrol., v. 27, p. 343-396.

Greenwood, H.J., 1976, Metamorphism at moderate temperatures and pressures. in The Evolution of Crystalline Rocks, eds. Bailey, D.K. and MacDonald, R., Academic Press, New York, p.187-259.

Guidotti, C.V., 1970, The mineralogy and petrology of the transition from the lower to the upper sillimanite zone in the Oquossic area, Maine. Jour. Petrol.,v. 11, 277-336.

Halliday, A.N., Stephens, W.E., and Harmon, R.S., 1981, Isotopic and chemical constaints on the development of peraluminous Caledonian and Acadian granites, Can. Mineral., v.19, 205-216.

Haselton, H.T. and Newton, R.C., 1981, Thermodynamics of Pyrope-grossular garnet and their stabilities at high temperatures and pressures, in Special Issue honoring George Kennedy, Boetcher, A.L. compiler, Jour. Geophys. Res., v. 85, p. 6973-82.

Hensen, B.J., 1987, P - T grids for silica-undersaturated granulites in the system MAS (n + 4) and FMAS (n + 3) - Tools for the derivation of P - T paths of metamorphism. Jour. Met. Geol., v. 5, p. 255-271.

Hewitt, D.A. and Wones, D.R., 1984, Experimental phase relations of the micas, in Reviews in Mineralogy, Micas, Ribbe, P.H., ed., Bookcrafters Inc., Chelsea, MI, p. 201- 256

Hills, F. A. and Armstrong, R.L., 1974, Geochronology of the Precambrian rocks in the Laramie range and implications for the tectonic framework of Precambrian southern Wyoming, Precambrian Research, v. 1, p. 213-225.

Hodge, D.S., 1966, Petrology and structural geometry of Precambrian rocks in the Bluegrass Area, Albany County, Wyoming, Unpubl. Ph.D., Univ. Wyoming, 135 p.

Hodge, D.S. and Mayewski, P.A., 1969, Gravity study of a hypersthene syenite in the Laramie Anorthosite Complex, Wyoming., Geol. Soc. Amer. Bull. v. 80, p. 705-714.

Holdaway, M.J., 1971, Stability of andalusite and the aluminosilicate phase diagram. Amer. Jour. Sci., 271, 97-131.

Holdaway, M.J., and Lee, Sang Man, 1977, Fe-Mg cordierite stability in high grade pelitic rocks based on experimental, theoretical, and natural observations, Contrib. Mineral. and Petrol., v. 63, p. 175-198.

Houston, R.S., Karlstrom, K.E., Hills, F.A., and Smithson, S.B., 1979, The Cheyenne Belt - The major Precambrian crustal boundary in the western United States, GSA abstracts with programs, v.11, p.446.

Jaeger, J.C., 1964, Thermal effects of intrusions, Rev. Geophysics, v.2, No. 3, p. 443-466.

_____, 1968, Cooling and solidification of igneous rocks, in, Basalts: The Polervaart Treatise on rocks of basaltic composition, H.H. Hess and A. Poldervaart (eds.) 2, 503-536, Wiley-Interscience, New York.

Klugman, M.A., 1960, Laramie anorthosite, guide to the geology of Colorado, Denver Geol. Soc. of America, Rocky Mountain Assoc. Geologists, Colo. Scientific Soc., p. 223-227.

Levin, E.M., Robbins, C.R., and McMurdie, H.F., 1968, Phase Diagrams for Ceramists, The American Ceramic Society Inc., Columbus, Ohio.

Mehnert, K.R., Busch, W., and Schneider, G., 1973. Initial melting at grain boundaries of quartz and feldspar in gneisses and granulites. M. Jb. Miner. Mh. 1973, 165-83.

Newhouse, W.H., and Hagner, A.F., 1945, Structure of the Laramie Range anorthosite, Wyoming (abs.), Geol. Soc. Amer. Bull., v. 56, p. 1184-1185.

_______ 1947, Zoned metasomatic gneisses related to structure and temperature, Laramie Range, Wyoming (abs.), Geol. Soc. Amer. Bull., v. 58, p. 1212-1213

Newton, R.C., 1983, Geobarometry of high-grade metamorphic rocks, Amer. Jour. Sci., v. 283-A, p. 1-28.

Ohmoto, H., and Kerrick, D., 1977, Devolitization equilibria in graphitic systems. Amer. Jour. Sci., v. 277, p. 1013-1044.

Peterman, Z.E. and Hedge, C.E., 1968, Chronology of Precambrian events in the Front Range, Colorado, Can. Jour. Earth Sci., v. 5, p. 749-756.

Phillips, G.N., Wall, V.J., and Clemens, J.D., 1981, Petrology of the Strathbogie batholith: a cordierite bearing granite, Can. Mineral., v.19, 47-64.

Putnis, A. and Holland, T.J.B., 1986, Sector trilling in cordierite and equilibrium overstepping in metamorphism. Contrib. Mineral. Petrol., v. 93, p. 265-272.

Reinhardt, E.W., 1986, Phase relations in cordierite-bearing gneisses from the Gananoque area, Ontario, Can. Jour. Earth Sci., v. 5, p. 455-482.

Rice, J.M., 1983, Metamorphism of rodingites: Part I, Phase relations in a portion of the system CaO-MgO-Al_2O_3-SiO_2-CO_2-H_2O. Amer. Jour. Sci., v. 283-A, p. 121-150.

Richardson, S.W., 1968, Staurolite stability in a part of the system Fe-Al-Si-O-H, Amer. Jour. Sci., v. 267, p.259-272.

Schreyer, W., 1976, Experimental metamorphic petrlogy at low pressures and high temperatures, in The Evolution of Crystalline Rocks, eds. Bailey, D.K. and MacDonald, R., Academic Press, New York, p. 261-331.

______, and Seifert, F., 1969, Compatibility relations of the aluminum silicates in the system MgO-Al_2O_3-SiO_2-H_2O and K_2O-MgO-Al_2O_3-SiO_2-H_2O at high pressures, Amer. Jour. Sci., v. 267, p. 371-388.

Seifert, F., 1976, Stability of the assemblage cordierite + K-feldspar + quartz, Contrib. Mineral. Petrol., v. 57, 179-185.

Skippen, G.B., 1971, Experimental data for reactions in siliceous marbles. Jour. Geol., v.79, p.457-481.

_______, 1974, An experimental model for low pressure metamorphism of siliceous dolomitic marble, Amer. Jour. Sci., v. 274, p. 487-509

Snyder, G.L., 1984, Preliminary geologic maps of the Central Laramie Mountains, Albany and Platte Counties, Wyoming, Open file report 84-358 (parts A through M).

Speer, J.A., 1985, Metamorphism of the pelitic rocks of the Snyder Group in the contact aureole of the Kiglapait layered intrusion, Labrador: effects of buffering partial pressures of water, Can. Jour. Earth Sci., v. 19, p. 1888-1909.

Spry, A. 1969, Metamorphic Textures, Pergammon Press Inc. Elmsford, N.Y., 350 p.

Strong, D.F., and Hanmer, S.K., 1981, The leucogranites of southern Brittany: origin by faulting, frictional heating, fluid flux and fractional melting, Can. Mineral., v.19, 163-176.

Thompson, A.B., and Algor, J.R., 1977, Model systems for anatexis of pelitic rocks, Contrib. Mineral. Petrol., v. 63, p. 237-269.

Torres-Rolon, R.L., 1983, Fractionated melting of metapelite and further crystal-melt equilibria - The example of the Blanca Unit migmatite complex, north of Estepona (Southern Spain), Tectonophysics, v. 96, p. 95-123.

Tracey, R.J., 1978-A, Partial melting in pelitic schist, Amer. Jour. Sci., v. 278, p. 150-178.

_______, 1978-B, High grade metamorphism and partial melting in pelitic schist, west-central Massachusetts, Amer. Jour. Sci., v. 278, p. 150-178.

Trommsdorff, V., and Evans, B.W., 1977, Antigorite - ophicarbonates: Contactact metamorphism in Valmenco, Italy, Contrib. Mineral. Petrol., v. 62, p. 301-312.

Tuttle, O.F., and Bowen, N.L., 1958, Origin of granite in light of experimental studies in the system $NaAlSi_3O_8$ - $KAlSi_3O_8$ - SiO_2 - H_2O: Geol. Soc. Amer. Mem. 74, 153p.

Tyler, I.M. and Ashworth, J.R., 1982, Sillimanite - potash feldspar in graphitic pelites, Strontian Area, Scotland, Contrib. Mineral. Petrol., v. 81, p. 18-29.

Vernon, R.H., 1987, Growth and concentation of fibrous sillimanite related to heterogeneous deformation in K-feldspar - sillimanite meta-pelites, Jour. Met. Geol., v. 5, p 51-68.